POLITECNICO DI TORINO
Repository ISTITUZIONALE

Assessing the role of fluctuating renewables in energy transition: Methodologies and tools

(Article begins on next page)

14 November 2024

Assessing the role of fluctuating renewables in energy transition: methodologies and tools

Ettore Bompard[1,2], Alessandro Ciocia[1], Daniele Grosso[2,3], Tao Huang[1,3] *, Filippo Spertino[1],

[1] Department of Energy, Politecnico di Torino, Turin, Italy

[2] LINKS Foundation, Turin, Italy

[3] Energy Security Transition (EST) Lab@energycenter, Politecnico di Torino, Turin, Italy

Mehdi Jafari, Audun Botterud

Laboratory for Information and Decision Systems, Massachusetts Institute of Technology,

Cambridge, USA

jafari@mit.edu, audunb@mit.edu

Abstract— Due to the environmental impacts brought by current energy schemes, the energy transition, a new paradigm-shift from fossil fuels to renewable energy, has been widely accepted and is being realized through collective international, regional, and local efforts. Electricity, as the most direct and effective use of renewable energy sources (RES), plays a key role in the energy transition. In this paper, we first discuss a viable pathway to energy transition through the electricity triangle, highlighting the role of RES in electricity generation. Further, we propose methodologies for the planning of wind and solar PV, as well as how to address their uncertainty in generation expansion problems. Finally, by using a web-based tool, "RES-PLAT"[1], we demonstrate the scheme in a case study in Egypt, which evaluates the impacts and benefits of a large-scale RES expansion.[2]

Keywords—energy transition, generation expansion, RES planning, res-plat, uncertainty, North Africa

I. INTRODUCTION

The energy transition, which is characterized by the shifting from fossil-based energy and economic schemes towards renewable-based ones, is gaining momentum at the global scale. Actions have been taken at different levels (policy, regulatory, technological) in various countries to achieve the decarbonisation targets in order to ensure a sustainable and secure future energy system and economy.

Electricity, as the most direct and effective use of renewable energy sources (RES), stands at the center of the energy transition. To concretely ensure a positive impact with respect to the energy transition goals, the link among the electricity generation from RES, the transmission

---

[1] https://res-plat.est.polito.it

[2] The short version of the paper was presented at Applied Energy Symposium: MIT A+ B, August 13-14, Boston. This paper is a substantial extension of the short version of the conference paper.

and distribution of energy in the form of electricity, and electrification at the final energy use (the so-called "electricity triangle") is needed [1]. In this triangle, in particular, cost-effective integration of RES into the electricity system is vital to guarantee energy security, affordability, as well as sustainability.

In general, in fact, different choices and, consequently, different long-term pathways related to the energy transition produce multi-dimensional effects (i.e., the impact on the energy systems, on the environment, on the economy, and on the society). For this reason, it is important to develop science-based methodologies and planning tools that can quantitatively provide a holistic assessment of these impacts.

In literature, some methodologies are presented for the planning of RES. The work in [2] studies the optimization of the sizes of renewable sources and storage technologies in the electric grid, with a focus on the optimization algorithm. In particular, this paper proposes a two-stage planning framework based on fuzzy multi-criteria-decision-making techniques to select the most promising RES-storage portfolio. Other papers [3][4] work on the same aspect; nevertheless, they do not deal with the issue related to the localization of the sources or the problem of the spatial-temporal variability of the sources.

Another important topic is the planning and management of transmission grids in scenarios with high renewable penetration. For example, the paper [5] presents a methodology to assess the amount of RES generation to be curtailed to avoid overloads due to grid congestions, helping in increasing the acceptable grid capacity. Similarly, the paper [6] proposed an inter-regional energy delivery planning model considering the uncertainties of wind and photovoltaic, to minimize the overall cost. An interesting aspect is that in this paper, the different scenarios are created after the study of historical data of renewables production. In these cases, the attention is focused on the electric grid, while analysis from the side of the RES potential is missing.

A holistic RES planning procedure is presented in [7]; in this work, there is a brief description of the main steps for the planning of large-scale renewable, but with no practical example and no RES potential analysis. On the contrary, the paper [8] presents a case study related to the planning of the electrical energy system with a high share of renewable supply for Portugal, supported by a methodology and a tool. The methodology starts with the import of load and generation profiles, system operating cost, etc. The optimization is performed to maximize the use of renewables or to minimize the grid cost and the output of the procedure are the analysis of the scenarios indexes for different sizes of generators.

The tool EnergyPLAN [9] is used to perform the balances in the grid in [8]; it optimizes sizes and calculates all the balances. This software permits to quickly calculate the effect of complex scenarios, including any kind of generation, based on hourly basis time series. Another software with similar characteristics is [10]. The main drawback is that they focus only on the energy and financial aspect of the planning, without taking into account all the technical aspects related to the potential of the RES sources in different regions. On the contrary, other tools/platforms are specialized in the analysis of the RES potential on a GIS

basis; they permit to apply some criteria for the selection of the most suitable sites. For example, in [11] PVGIS and document [12] provide maps of irradiance and permit to calculate the production from PV systems. [13] and [14] provide maps of wind speed for the installation of wind turbines with info about production potential; it is worth noting that [13] also provides maps of terrain roughness, which is one of the most important criteria for the planning of this technology. These platforms are not built to perform the optimization of the sources, to analyze and compare scenarios, for example with different storage capacities and grid constraints.

In this paper, an interdisciplinary methodology for RES planning focused on wind and solar photovoltaic technologies is proposed; the framework is able to assess the energy productivity of different technologies with reference to different spatial scales (from single sites to countries). This approach allows to perform a pre-screening of the possible locations for RES plants installation, based on several criteria taking into consideration the topographic characteristics of the sites themselves, thus strongly coupling geomatics and energy analysis. The result is the definition of the most suitable areas/site for the development of each different RES technology at the regional, national and international levels. Furthermore, in the proposed procedure, it is shown how to take into account inter-annual variability and uncertainty of RES in the system planning and operation problem using multiple years of RES data, and find optimal solutions for the generation system configuration, which is robust over different weather years.

In particular, hourly power profiles are calculated starting from weather data (irradiance, air temperature, and wind speed), the roughness of the installation site, and other key factors, such as thermal losses for PV generators and efficiency of electronic converters. The calculations also consider the wind speed-power output curves to compare different commercial turbine models and define the best wind turbine in each location if the terrain is not too complex. Finally, a comparison between production profiles and consumption profiles permits us to define the best portfolio of photovoltaic plants and wind turbines.

As for the uncertainty of RES in the generation expansion, instead of relying on a single year of time series data, it is important to optimize the system for multiple years of renewable and load data to ensure robust operation of the system across different weather years.

Finally, we apply the models implemented in the "RES-PLAT"; the platform has been developed at the EST@ Energy Center – PoliTO Lab to Egypt, as a case study, to quantitatively evaluate the RES exploitation potential and the exporting possibility to Europe based on a set of scenarios.

II. THE ROLE OF ELECTRICITY IN THE ENERGY TRANSITION

A. Energy Transition

The crucial role of energy in society is a well-received concept, and its availability is an important indicator of the level of welfare of nations and social communities, from survival

to prosperity. After centuries of development, the current world energy system depends heavily on fossil fuel and fosters several issues that need to be addressed.

GHG emission: Energy accounts for 2/3 of global greenhouse gas (GHG) emissions [15]. In 2017 fossil fuels accounted for 81.3% of the global Total Primary Energy Supply (TPES), which produced 32.8 Gt CO_2 emissions - an increase of 60% w.r.t. 1990. The US, EU, Russia, China, India, and Japan accounted for about 67% of the overall CO_2 emissions [16]. Consequently, climate change becomes increasingly evitable and concerning. For example, the global land and ocean surface temperature increased 0.85 °C over the period 1880-2012, the Arctic sea-ice extent reduced 3.5÷4.1% per decade over the period 1979-2012, and the global mean sea level increased 0.19 m over the period 1901-2010 [17]. The strong increase in the anthropogenic emissions w.r.t. the pre-industrial levels has led to atmospheric concentrations of CO_2, CH_4, and N_2O that have not been reached in the last 800,000 years [17]. Through international negotiations, the Paris agreement aims to make sure the increase of the global average temperature will be held well below 2°C above pre-industrial levels [18].

Air pollution: The use of energy commodities is responsible for the majority of pollutant emissions, according to [19], more than 99% of SO_2 and NOX, 90% of CO, 80% of PM2.5, and 60% of VOC are emitted from the use of energy commodities. These have a large and negative impact on the well-being of people around the world. The estimation from IEA said that in 2012, the world deaths that can be attributed to air pollution were 7.3 million and the cumulative years of life lost were about 262 million years [19].

Depletion of fossil fuels: The fossil resources are not inexhaustible. At the current consumption rate, the proven reserves of fossil fuels will be depleted within around a century: more specifically, gas and oil will be gone in about 50 years, and coal will be depleted in 130 years, according to [20].

These factors are critical drivers for the energy transition. The energy transition is the mid/long-term transition of energy systems towards decarbonization, i.e., with a shift of the energy mix from fossil fuels to renewable energy sources (hydro, solar, wind, geothermal, biomass, tidal). Even if nuclear could be an option for the baseload, and it is carbon-free, its share in the electricity generation is expected to remain limited (6.1-11.7% by 2050, according to [21]).

B. Electricity triangle

RES has a huge theoretical resource potential, in principle be able to cover the global energy needs by a wide margin. According to the survey in [22], the long-term potentials of electricity generated from RES are between 1340–14,780 EJ/y for PV, 250–10,790 EJ/y for concentrated solar power (CSP), 350–1800 EJ/y for onshore wind, 1000–3050 EJ/y for the overall wind (both onshore and offshore), 118–1109 EJ/y for geothermal, and 53 EJ/y for hydro. Considering the global TPES of 585 EJ in 2017, it can be satisfied by the solar flux reaching the Earth in less than 2 h [23]. Therefore, if it is possible to tap into the huge

availability of these resources, electricity can be generated entirely from RES, achieving the carbon-free economy targeted by the energy transition.

However, converting RES to electricity alone is not enough. It only solves the problem on the electricity production side. Two additional elements are needed to implement the electricity-based energy transition, i.e., the transmission of electricity as an energy vector and electrification of final energy. The triangle formed by these 3 fundamental elements for energy transition is called the electricity triangle.

- Power generation directly from renewable energy sources, mainly wind and solar, replacing generation from fossil fuels;
- Use electricity as an energy carrier, transporting energy through power transmission and distribution infrastructures, thus taking advantage of high efficiency, low losses, and instantaneous transport.
- Electrification of energy end-uses to provide needed services with higher efficiency than other energy commodities.
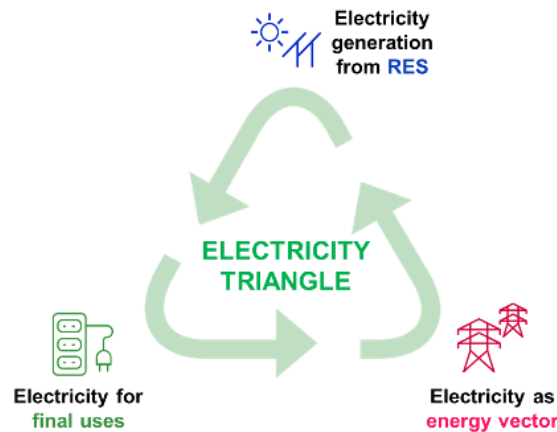

Fig. 1. Electricity triangle

Moreover, due to RES variability, energy storage systems (ESS) are key elements to keep the secure operation of the electricity systems. This includes technologies to ensure power quality (fast release of power in a short time), like electrochemical storages, super-capacitors, electro-mechanical systems; technologies providing frequency regulation services (e.g., "cold" and "warm" electrochemical storages for Frequency Containment Reserve (FCR), flow batteries and compressed air energy storage for Frequency Restoration Reserve); and long-term storage (pump-hydro plants and new approaches like Power-to-X).

In addition, electricity from RES has to communicate with other commodities, at least in short to mid-term. The cross-vector interplays among electricity, hydrogen, and gas are crucial. For example, the implementation of Power-to-Gas technologies for long-term storage, optimally exploiting the excess of electricity from RES and avoiding curtailments, etc., need well-designed interoperable multi-energy systems.

Considering the complexity of the energy transition, the RES deployment needs planning capable of matching technical aspects with sustainability issues and the economic feasibility

of the investments. Therefore, science-based tools for decision-making support through comprehensive analyses and impact assessment are indeed needed.

III. AN INTERDISCIPLINARY PROCEDURE FOR THE ASSESSMENT OF THE RES POTENTIAL

Photovoltaic (PV) generators and Wind Turbines (WT) are today the most used renewable energy technologies in the world due to several reasons. First, the exploitation of solar and wind energy does not present issues related to scarcity in many locations. In addition, from a financial point of view, the return on investment of PV and wind power is high and, above all, increasing (unlike most fossil fuels). Another key aspect is the huge availability of raw materials (like silicon) in the Earth's crust. Then, especially for PV modules, the structure of the devices is compact, and the thermal load and mechanical stresses are much lower than other technologies; thus, maintenance is not an issue. For these reasons, the levelized cost of solar energy is lower with respect to other technologies in many countries. Therefore, in this section, an interdisciplinary methodology for the planning of solar PV systems and wind turbines is introduced.

The stakeholders involved in the planning of RES are multiple. Governments should drive the transition to renewables by creating policies in their favor, according to economic and political constraints. Banks and financial institutions look for the best solutions in order to focus their financial effort on the most promising projects. Companies and citizens need to know how to integrate the renewable system to reduce the use of fossil fuels and increase their independence from the grid. All of these stakeholders have a common goal: to know which renewable energy sources are the most suitable from energy and economic points of view. To answer this question, it is necessary an interdisciplinary procedure and its methodological innovation consists of the approach in which the following aspects are combined together in a harmonic way: geographic aspects, electrical energy and economy, engineering and architecture in urban and rural areas, environment, human societies.

Given the complexity of the objective to reach, the procedure should be a compromise between accurate models and first approximation calculation to permit all the stakeholders to access these kinds of information with an acceptable understanding.

The first step of the procedure defines the criteria for the selection of the most suitable areas for each RES technology. Using solar photovoltaic and wind turbines as an example, it is required to have at disposal weather data in order to identify the sites with the highest solar irradiation and wind speed, thus the most promising in terms of energy production. Besides the weather data analysis, the study of terrain morphology is of fundamental importance for the correct planning, such as taking into account the connection with the electric grid and the proximity to electric loads (cities, industrial parks, etc.) to increase their self-sufficiency.

The second step involves the calculation of power profiles and energy parameters, such as the productivity of the plants. It requires the analysis of the weather data, the selection of the most appropriate technology, depending on the results obtained in the previous step. The mathematical models shall be appropriate for the proposed task of defining suitable sites,

avoiding a too high complexity (to reduce the consequent computational burden in case of surfaces as large as entire nations), but with accurate results. In the present work, the comparison of two PV models is presented, and the difference in energy estimations is quantified. Regarding wind generation, three typologies of wind turbines are considered, and the differences in their energy production are quantified.

Fig. 2. An Interdisciplinary Procedure for the Assessment of the RES Potential

The third step involves the management of the uncertainty from RES. It is related to several factors, starting from the quality and accuracy of the inputs of the models, the RES forecast uncertainty in operating reserve requirements and system dispatch, and the flexibility characteristics of generation, demand, and energy storage. In the present work, the formulation of the optimization problem is presented, with the focus on the importance of the use of multiple years of weather data inputs.

Finally, the last step works with the definition of an architecture of an information system necessary to manage the massive quantity of data necessary for the planning of RES at the regional, national, and international levels. In the present work, the case of the RES-plat is briefly described as the practical implementation of the proposed procedure.

As a result, the output of the procedure is the power profiles of RES plants and their localization, the qualification of economic and environmental benefits, and the creation of data scenarios useful for the development of the energy transition. A description of the steps of the procedure is presented in the following subparagraphs; the application of the procedure is presented in the case study of Chapter IV.

A. Criteria for the selection of suitable sites for RES

In future energy systems, the combination of utility-scale PV systems, wind farms, and a smaller quota of residential PV systems will cover a great part of the electric loads.

Utility-scale PV systems are characterized by sizes in the range of 100–1000 MW (and even bigger). These plants can be installed in wide semiarid zones not usable for other activities (e.g., farming). From the technological point of view, the PV generators are equipped with Sun-tracking systems (single or double axis) to follow the apparent path of the Sun: this permits a yearly increase of production of >30% with respect to fixed systems and lower seasonal variations. Currently, the single-axis tracking system is the most used in utility-scale PV plants; it is the optimal compromise between the production gain and the maintenance costs. Thanks to the increase in efficiency and even lower costs, these systems are supposed to gain market share, even with respect to wind farms.

A contribution is due to PV plants of low-medium sizes (from few kilowatts to several megawatts); they are installed on the rooftops of buildings and permit to produce directly where the electric loads are placed.

The maximum current efficiency of commercial crystalline silicon (mono and poly) modules is about 20%, but in the midterm, the target for this technology goes beyond the 30%-threshold. The occupation of soil both direct for equipment and indirect for suitable spaces to avoid mutual interference is assumed as follows. For utility-scale PV systems, a nominal efficiency of 20% is assumed, leading to an area of 5000 m^2 necessary to install a rated power of 1 MW. A multiplicative factor equal to 2 is assumed to reduce the mutual shadows between the rows of modules in fixed systems, while a multiplicative factor of 3 is assumed for solar tracking systems.

Wind farms, currently composed of wind turbines with a rated power of 2-3 MW (or more), can reach power ratings up to gigawatts. They also generate during night hours and help the PV systems to provide renewable power with less daily variations. The rotor diameter of wind turbines is currently longer than 110 m, and the hub height is taller than 100 m, but both dimensions will be increased by some tens of meters to maximize energy production. The performance enhancement depends only on the size as the conversion efficiency is already very close to the Betz limit (about 59%) in the speed range where it is permitted to track the maximum wind power.

Regarding the land use for wind turbines, the area swept is about 2300 m^2 for a turbine with a rated power of 1 MW; moreover, to reduce mutual interference, 2 space factors must be adopted. The first space factor is equal to 3÷5 times the diameter of the rotor for the direction normal to that prevailing of the wind. The second space factor is equal to 7÷10 times the diameter of the rotor for the prevailing wind direction.

In conclusion, the total land use is higher for wind than for PV. In the near future, the enhancement in the conversion efficiency of PV modules and the safe usage of larger wind rotors and taller hub heights will reduce the land cover per unit of installed power.

A correct procedure for the planning of RES requires criteria that can be divided into two macro-categories, closely related to each other: technical feasibility and cost-effectiveness. In fact, the PV+WT plant sites should be chosen in order to ensure both the feasibility of the installation from a technical perspective and satisfying installation and Operation and Maintenance (O&M) costs [24]. For example, the installation requires particular attention in case of:

- too high slope of the terrain (<10° for wind turbines) which can cause high turbulence in the air stream, leading to excessive mechanical stress and energy underperformance, as clarified in the subsection dedicated to the wind power model. Moreover, transportation of turbine blades, towers, and nacelles might be difficult. For parts being transported by road, their big size means a route planning and could require route improvements, such as the increase of the road width and the removal of trees and other obstacles;

- excessive altitude of the sites: extreme weather conditions can damage the WT blade and drive train materials. The altitude limit depends on the climate and geographical location in a country/region and on the characteristics of the turbines. As an example, one of the

most important manufacturers of wind turbines in the world suggests considering a reference limit in the range of 1000—1500 m for 2MW turbines [25]. Above this limit, special considerations must be taken regarding, for example, snow and icing, that can affect the performance of wind turbines and High Voltage (HV) installations;

- harsh weather conditions: e.g., in desert areas, sandstorms could damage PV glass and mechanical parts of wind turbines, strongly reducing their lifetime;

- for the PV generation, an appropriate share between the large-scale centralized power stations in low-value countryside (e.g., 70 % of the installed capacity) and the building applied or building integrated PV systems in urban areas to obtain the correct usage of the terrain;

- for the WT generation, an appropriate share between the onshore wind farms (e.g., 90 % of the installed capacity) and the offshore wind farms with the adequate spacing among the wind turbines to face with visual impact, roughness and complexity of the surface;

- high distance from the HV grid: if the grid connection point is not far from the wind farm, the connection is typically a high voltage alternating current (HVAC) connection. In the case of longer distances, a high voltage direct current (HVDC) line could be the best solution: the HVDC losses could be lower than in the case of HVAC, despite the losses in AC-DC conversion and vice versa. It has been estimated that HVDC connections can be favored for distances over 50 km [26]. The electrical work, electricity lines, and the connection point (including the transformer) to connect to a near HV grid are typically 11% to 14% of the total capital cost of onshore wind farms. In the case of longer distances, it can be much higher [27].

- self-sufficiency (*SS,* that will be defined in the sequel): the proximity of generation and loads allows to increase *SS* and to reduce the possibility of congestion and losses in the electricity grid. Thus, it is preferred to find installation sites that are close to cities, industrial parks, seaports, etc., particularly if these areas cannot be used for other purposes.

- proximity to special buildings and infrastructures (e.g., airports or military facilities);

- other factors such as terrain morphology not suitable for this kind of installations.

B. Calculation of RES productivity and power profiles

Modelling of solar photovoltaic production

The electrical performance of PV)generators can be accurately described by an equivalent circuit with lumped parameters. In the literature, the most used is the Single Diode Model (SDM), which is characterized by five parameters (Figure 2). For a PV cell, the DC output current I is obtained as a function of voltage V and of the photo-generated current I_{ph}, the reverse saturation current I_0, the series resistance R_s, the shunt resistance R_{sh}, and the p-n junction quality factor n [28].

$$I = I_{ph} - I_0 - (V + R_s \cdot I)/R_{sh} = \qquad (1)$$

$$= I_{ph} - I_0 \cdot \left(e^{\frac{q \cdot (V + R_s \cdot I)}{n \cdot k \cdot T_c}} - 1 \right) - (V + R_s \cdot I)/R_{sh}$$

In particular, I_{ph} is the production of the solar cell, while the second term is a source of loss, reducing the solar cell output current I. R_s is due to the front electrical contacts of the cell, while R_{sh} is due to the leakage currents flowing through the lateral surfaces of the cell.
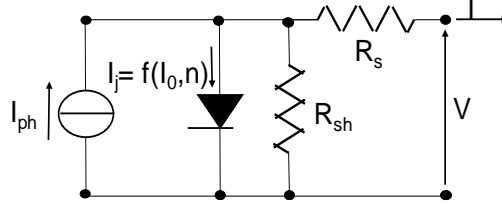

Fig. 3. Equivalent circuit of a PV cell.

Four of the five parameters of SDM are generally considered constant, while one is proportional to irradiance (I_{ph}). Recently, researchers are working to increase the accuracy of the model by considering a dependence on weather conditions of all the parameters. As shown in the equations from (1) to (4), I_{ph} and R_{sh} are, generally, assumed proportional and inversely proportional to irradiance, respectively; I_0 has an exponential dependence on temperature; R_s is mainly proportional to temperature; n has a weak linear dependence with irradiance and temperature.

$$I_0 = b \cdot \left(T / T_{STC} \right) e^{\left(\frac{1}{k} \left(\frac{E_{g,STC}}{T_{STC}} - \frac{E_g(T)}{T} \right) \right)} \qquad (2)$$

$$n = c \cdot G + d \cdot T \qquad (3)$$

$$R_s = e \cdot \left(T / T_{STC} \right) \cdot \left[1 + f \cdot \ln \left(T / T_{STC} \right) \right] \quad (4)$$

$$R_{sh} = g \cdot \left(G_{STC} / G \right) \qquad (5)$$

The optimization of the coefficients in the semi-empirical formulas is currently a hot topic in photovoltaic research. The optimization procedure in [29] requires the measurement of the current-voltage (*I-V*) characteristic curves of new and clean modules under different air temperature and irradiance conditions. This set of experimental curves is fitted with data from equations from (2) to (4). The parameters [*b c d e f g*] are optimized to minimize the differences between experimental data and the theoretical curves. Following the procedure in [29], the parameters for a crystalline silicon (c-Si) module at Standard Test Condition (STC, G=1000 W/m^2, T=25 °C) are shown in Table I.

TABLE I.   PARAMETERS FOR A C-SI MODULE AT STC - SINGLE DIODE MODEL

I_{ph} (A)	I_0 (A)	n (-)	R_s (mΩ)	R_{sh} (Ω)
9.06	$1.0 \cdot 10^{-7}$	1.2	4.02	$3.6 \cdot 10^7$

The procedure to obtain the output power using the SDM continues by using irradiance and PV module temperature as inputs in the equations from (1) to (5). Equation (1) must be repeatedly solved for a predefined set of voltage values, in order to create the *I-V* curve. The

power output P_{SDM} to store is the maximum power point (MPP) of the *I-V* curve that is continuously tracked by commercial PV converters. The number of points used as the set of voltage values for the definition of the I-V curve shall be sufficient to carefully define the I-V curve and correctly calculate the maximum power point. Regarding the solution of equation (1), it is transcendental; thus, its solution requires the use of numerical algorithms with iterations, analytical approximations, or graphical methods. [30].

In conclusion, the Single Diode Model carefully describes the operation of the photovoltaic generator; nevertheless, it implies a high computational burden in case of planning purposes, in which simulation could be performed for a high number of locations, entire areas, regions, and countries.

In order to obtain a simpler but sufficiently accurate model for planning purposes, the SDM, applied to clear sky days in the four seasons, is interpolated by a straightforward (STR) model including different types of losses in the energy conversion. Thus, from the current-voltage curve, it is profitable to establish a simpler model of PV power P_{str_m} proportional to irradiance G, by the rated conversion efficiency η_{STC}, the underperformance at low irradiance η_{lowG} and the thermal dependence η_{therm}. Regarding η_{STC}, the most important worldwide manufacturers sell crystalline silicon modules with a typical efficiency of up to $\approx$21% [31][32][33]. The low irradiance losses are incorporated in η_{lowG} that has a dependence on irradiance only at low irradiance by the factor $G_0 \approx 20 \div 40$ W/m^2 [34]. The thermal dependence on the PV performance η_{therm} is a function of module temperature and the thermal factor $\gamma_{therm} \approx 0.35 \div 0.45\%/°C$ [31][32][33].

$$P_{STR} = \eta_{STC} \cdot \eta_{lowG} \cdot \eta_{therm} \cdot G \qquad (6)$$

with $$\eta_{lowG} = 1 - G_0/G \qquad (7)$$

$$\eta_{therm} = 1 - \gamma_{therm} \cdot (T - 25°C) \qquad (8)$$

Figure 4 shows the nonlinear dependence of the PV generator efficiency as a function of irradiance and temperature. In particular, the PV efficiency is quite constant for high irradiance values (G>600 W/m^2), while it strongly decreases in the case of G<200 W/m^2.
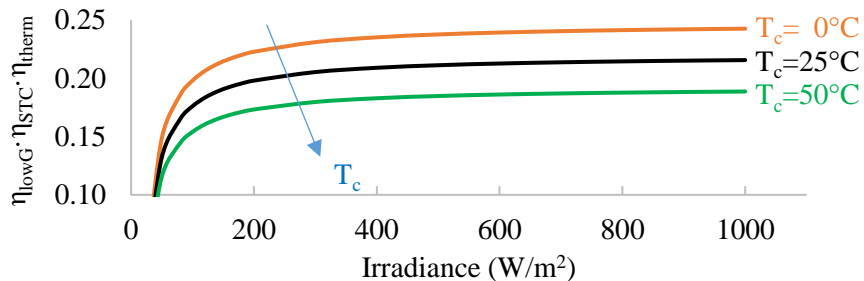

Fig. 4. PV efficiency as a function of irradiance and temperature - straightforward model.

The comparison between the SDM and STR models is shown in Figure 5. The power values P_{SDM} and P_{STR} are obtained from the same set of irradiance and air temperature data, which refer to a site with a Mediterranean climate (Rome). The data are sorted from smallest to largest, and it is worth noting that the main differences are concentrated in the higher values. As a result, the straightforward model is conservative with respect to the SDM, and

the annual energy deviation is about -3,6%. Table II shows the deviations of the STR with respect to the SDM in three sites with different irradiations and air temperatures; in every case, the deviation is lower than -4%. This deviation is within the uncertainty for irradiation measurements with commercial sensors based on reference solar cells [35][36].
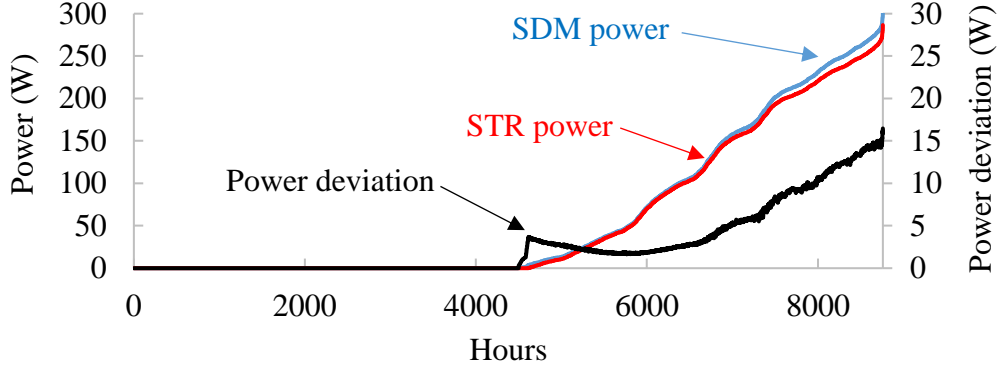

Fig. 5. PV production as function of irradiance – straightforward vs. single diode model .

TABLE II.   ENERGY DEVIATION IN DIFFERENT SITES – STRAIGHTFORWARD VS. SINGLE DIODE MODEL

Site	Yearly horizontal irradiation on PV modules (kWh/m²)	Yearly average air temperature (°C)	Energy deviation on annual basis
BERLIN	1076	10.3	-4,0%
ROME	1583	17.1	-3.6%
CAIRO	2075	21.2	-3,8%

After the computation of the power from the straightforward model, the AC production is calculated. The AC power depends on the non–linear efficiency in the DC/AC conversion (the commutation and conduction losses are taken into account in the calculation of $\eta_{DC/AC}$), and the other sources of losses $\eta_{mix}=(1 - \xi_{mix})$.

$$P_{AC} = \eta_{STC} \cdot \eta_{lowG} \cdot \eta_{therm} \cdot \eta_{DC/AC} \cdot \eta_{mix} \cdot G \qquad (9)$$

The above-described model does not take into account the effect of wrong design or installation. The worsening of performance in building applied PV systems due to shadowing is accurately defined in [37].

Modelling of wind turbine production

The calculation of production from wind turbine involves the wind speed distribution and the manufacturer's power curve of the turbine, which is the relationship between the wind speeds and the AC power output. Before using the power curve of the turbine, it is necessary to transfer wind speed to the height of the turbine hub by the following equation, depending on terrain roughness length z_0:

$$u_w = u_{ref} \cdot \frac{ln\left(z/z_0\right)}{ln\left(z_{ref}/z_0\right)} \qquad (10)$$

where u_w is the wind speed (m/s) at the height z of the hub (m), u_{ref} is the wind speed (m/s) measured at the height of the weather station z_{ref}, and z_0 is the roughness length. Roughness

is low in the case of water, and it is high for complex terrains, such as mountains or cities with tall buildings and skyscrapers [38].

For the correct planning of wind farms, the best turbine should be selected for each specific location. The selection is performed comparing the performance of different commercial wind turbines. For each wind speed value, the global efficiency of each wind turbine is calculated as the ratio between the electric power output and the aerodynamic wind power:

$$\eta_{WT}^{glob} = u_{ref} \cdot \frac{P_{el}^{WT}}{0.5 \cdot A \cdot \rho_{air} \cdot u_W^3} \qquad (11)$$

where u_W (m/s) is the wind speed at the height z of the rotor hub, passing through the swept area A (m^2) of the three-blade disk (perpendicular to the wind speed), a function of the blade length.
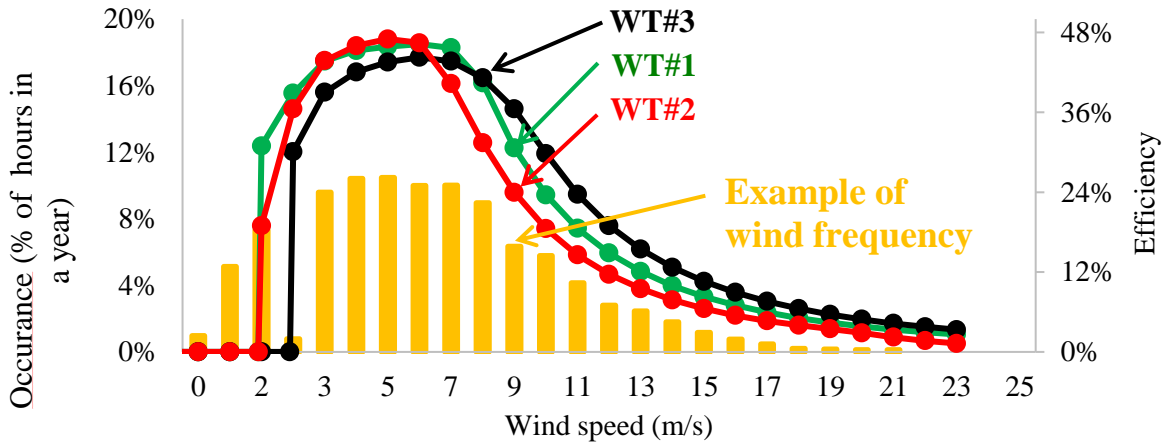

Fig. 6. Comparison between three WTs with different characteristics

Figure 6 illustrates an example of wind speed distribution for a site in a North Africa country, in which the efficiency curves of three different turbines are compared. In this site, the first turbine (WT#1) has the best performance; it has the largest rotor and the tallest hub height permitting the extraction of the highest energy at low wind speed. The turbine (WT#2) has average performance with the same rotor as in the case of WT#1 and lower hub height. The last turbine is a device designed for higher wind classes (WT#3) with long life; it has the lowest performance but less maintenance than the others.

Table III shows an example of energy productivity assessment for the three above defined wind turbines. The same three sites in Table II are used for the comparison. The early average wind speed is calculated at the height of the weather station (10 m), while the production is calculated after the wind speed transfer by (10) at the height of each turbine hub. In every case, WT#1 has the highest productivity, thanks to the higher efficiency for low wind speeds. With respect to WT#1, WT#2 has always a productivity ≈10% lower. WT#3 produced between -30% and -37% less than WT#1.

TABLE III. COMPARISON OF ENERGY PRODUCTION FOR DIFFERENT WIND TURBINE MODELS

Site		BERLIN	ROME	CAIRO
Yearly average wind speed (m/s)		3.9	3.2	3.5
Productivity (kWh/kW/year)	WT#1	3274	1645	2571
	WT#2	2970	1460	2257
	WT#3	2331	1062	1613

This procedure is effective in the assessment of the energy production, only if the terrain is flat or with simple morphology. On the other hand, in the case of complex terrain (mountains with ridges and valleys), the calculated energy may be much higher than the real production. This issue is clarified by Figure 7, where a WT installed on complex terrain produces only less than 80 % of the productivity calculated by the above-described procedure [38]. The experimental data are corrected according to a statistical method validated on windy Italian sites. This amount of underperformance is a sufficient reason to discard locations with complex terrain.
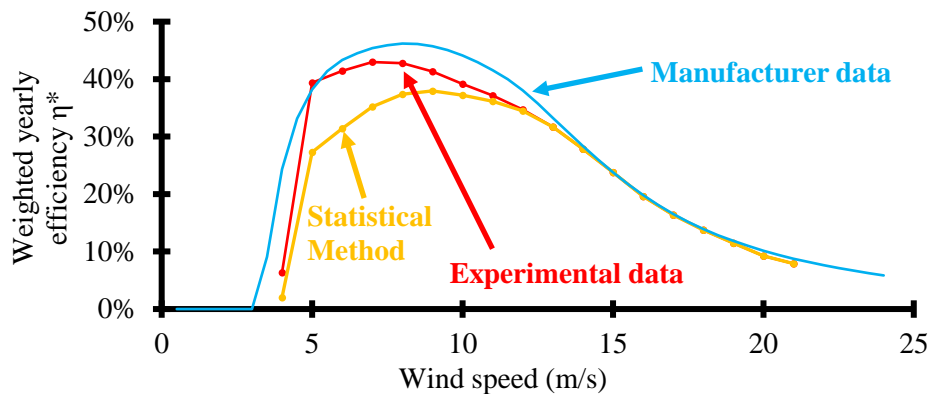

Fig. 7. Weighted yearly efficiency of a wind turbine in case of complex terrain – manufacturer data vs. experimental data

Time step of power profiles for the planning of RES

The planning of local renewable systems is based on the comparison of local generation and electric loads profiles. This comparison leads to the calculation of the exchanges with the grid and permits the sizing of a potential storage systems. Two indicators are used for the optimal sizing of local generators: self-sufficiency (*SS*) and self-consumption (*SC*). *SS* is the ratio between the electricity locally generated and consumed, and the total local consumption [39]. *SC* is an indicator similar to *SS*, and it is the ratio between the electricity locally generated and consumed, and the total generation. Both high *SC* and *SS* values are obtained when the local generation well matches the load profiles, leading to a reduced grid exchange [40].

For the calculation of energy flows and *SC* and *SS* indicators, production is generally computed using profiles with 1-h time steps [41]. Hourly profiles are easier to obtain, requiring a lower computational cost with respect to data per minute or second. For example, the hourly weather data provided by PVGIS [11] are already the results of data averaging and

elaboration of measurements performed with lower time step, according to the documentation in [42].

In most of European countries the balance settlement period is currently 1 h; only in the last years, the European Commission is working towards the harmonization and reduction to a common value of 15 min as balance settlement period [42]. The impact of time resolution (up to 1-h values) becomes almost negligible for the optimal sizing of PV generation, especially in the case of storage installation. In particular, the time step does not affect the sizing of PV system, while storage size can be affected by negligible errors (up to ≈2% in the case of 1-h time steps). From a financial point of view, the estimation of yearly savings on electricity bills results being affected by neither time resolution [43].

Figure 8 shows an example of consumption and generation profiles for a family in Italy. They are measured with a time step of 5 min. The 5-min profiles are averaged to obtain 1-h profiles, and the resulting graph is shown in Figure 9. The balance profile is the difference between local generation and load; thus, a negative balance is an absorption from the grid, while a positive balance is a surplus injected into the grid. The comparison of the two profiles demonstrates that a lower time resolution leads to the smoothing of the peaks and fluctuations.
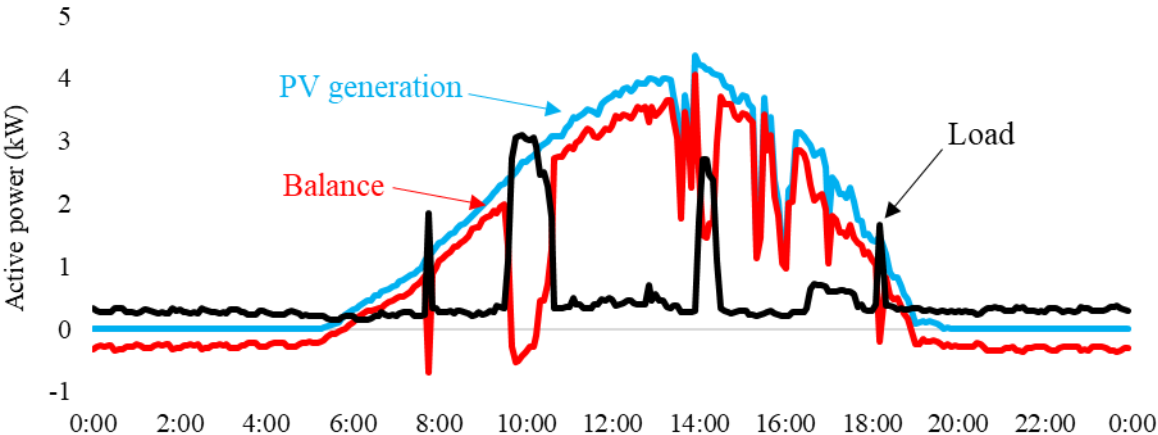

Fig. 8. Example of daily PV generation and load profiles with 5 min time step for a family in Italy
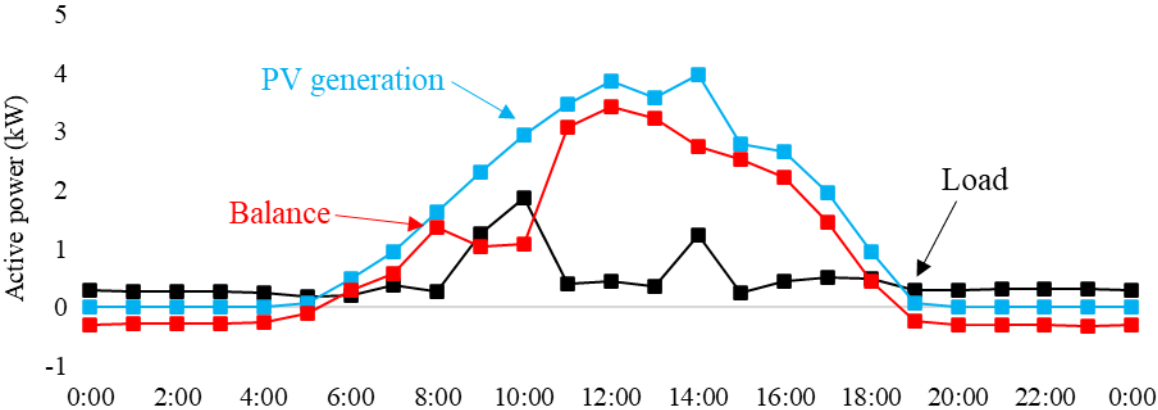

Fig. 9. Daily PV generation and load profiles with 1 hour time step resulting from the avering of the data in Figure 8

Obviously, the consumption and generation energies do not change at daily, monthly, and yearly levels by varying the time step of the profiles. The differences are in their balance, i.e. in the exchanges with the grid, generally leading to an overestimation of self-sufficiency and self-consumption. The deviations in the energy calculations related to the profiles in Figure 8 are quantified in Table IV. Self-sufficiency is 71% in the case of 5-min measured data; it increases to 73.8% hourly averaged profiles. Regarding self-consumption, it increases from 25% to 26% by using hourly data.

TABLE IV. PROFILES WITH DIFFERENT TIME STEPS: DAILY AND YEARLY ENERGIES AND BALANCES

	Single day		*Year*	
Time Step	*5 min*	*1 h*	*5 min*	*1 h*
Consumption (kWh/year)	11.2	11.2	6700	6700
PV generation (kWh/year)	31.8	31.8	5715	5715
Injection into the grid (kWh/year)	23.9	23.9	3318	3102
Absorption from the grid (kWh/year)	-3.2	-3.2	-4303	-4087
Self-sufficiency	71.0%	73.8%	35.8%	39.0%
Self-consumption	25.0%	26.0%	41.9%	45.7%

Table 2 also shows the same comparison performed on an entire year. In this example, thanks to a 6 kW PV plant, the yearly production is 5715 kWh/year; while the electric load is 6700 kWh/year due to standard appliances, induction cookers and a heat pump for hot water. By movign from 5 min measured data to hourly average values, injection in the grid decreases by 6.5%, while absorption from the grid decreases by 5%. As a result, on yeraly level, self-sufficiency increased by 3.2% and self-consumption increased by 3.8%. In conclusion, the proposed methodology is suitable for planning purposes; in fact, it is slightly affected by the use of hourly time steps.

Interannual variability of RES production

The planning of RES requires the analysis of the interannual variability in the electricity production. At this aim, it is necessary to use an adequate number of years of data for the renewable resources and the load consumption to correctly estimate energy and financial parameters. Regarding the solar resource, it is almost constant on a yearly basis all around the word, with variations that are generally lower than 4%. On the contrary, wind resource could have much higher deviations year by year, leading to the necessity of measurements for several years. Figure 10 shows an example of interannual variability analysis for PV and WT systems from 2005 to 2016. The chart displays the calculation of energy productivity of a PV generator and a wind turbine installed in Cairo. Both have a rated power of 1 MW. The ground mounted PV generator, installed with tilt 30° and South oriented, has an average productivity of 1818 MWh/MW/year, with a deviation of ±33 MWh/MW/year; thus, the production variability, calculated as the ratio between the standard deviation and the average value, is poor (±1.8%). The wind turbine (WT#1 type) has higher production in the first seven years, but lower in the last four years. Over the 12 years, the average wind turbine production

is 2238 MWh/MW/year, with a deviation of ±247 MWh/MW/year. In this case the WT production has a variability of ±11,0%. It is of note that the effect of ageing is not considered.
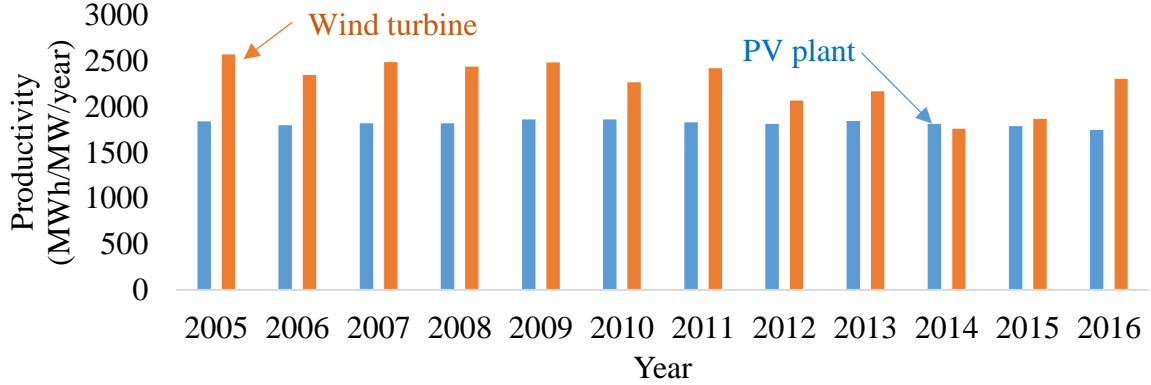

Fig. 10.   Example of interannual variability of RES production in Cairo, years from 2005 to 2016

The analysis performed in Cairo area is repeated for Rome and Berlin areas, and the results are shown in Table V. In every site, the PV plants are supposed South oriented and installed at the optimal tilt (e.g., 40° in Berlin and 35° in Rome).

TABLE V.   INTERANNUAL VARIABILITY OF RES PRODUCTION IN CAIRO, ROME AND BERLIN, YEARS FROM 2005 TO 2016

		Average productivity (MWh/MW/year)	*Deviation (MWh/MW/year)*	*Variability (%)*
CAIRO	PV	1818	±33	±1.8
	WT	2238	±247	±11.0
ROME	PV	1539	±52	±3.4%
	WT	2428	±964	±39.7%
BERLIN	PV	992	±50	±5.1%
	WT	3244	±408	±12.6%

The calculations for the additional sites confirm that the variability of PV generation is always much lower than the variability of wind generation: the maximum value for PV is in Berlin ($\approx \pm 5$ %), but the maximum value of variability for WT generation is the highest ($\approx \pm 40$ %) in Rome. As a conclusion, for the planning of PV systems, the use of few years of data can be acceptable; however, in case of wind turbines planning, the use of at least 10 years of data is suggested.

C. Assessment of the uncertainties for wind and PV generation profiles

A crucial point of concern is the assessment of the uncertainties linked to the profiles of PV+WT generation. These power profiles, to be realistic, depending on the accurate knowledge of the physical quantities of sun and wind. In particular, what are the actual values of uncertainty for the measurement of solar irradiance G and wind speed U_w? Looking at

recent literature on this topic [44][45][46], the minimum uncertainties are reached at peak values of these quantities corresponding to the rated power of the generators: $G = 1kW/m^2$ for PV generation and $U_w > 12$ m/s for WT generation. Considering the probabilistic approach with Gaussian distribution (coverage factor =2), these expanded uncertainties are about +/- 20 W/m^2 for G and +/-0.2 m/s.

The consequent impact on the calculation of produced power, knowing the efficiencies of energy conversion in the PV and WT generators, can be estimated taking into account that:

1. the PV power is directly proportional to irradiance;
2. the WT power depends on the cube of wind speed in the portion of the WT power curve, where the efficiency is almost constant and near the maximum value (range of more frequent wind speeds), while the WT power is almost independent of the wind speed if $U_w > 12$ m/s.

In conclusion, the simulated power profiles of PV+WT are affected by typical uncertainties that can be modeled in this simple way:

1. relative uncertainties = +/- 3% of the calculated values from 60% to 100% of the rated; power;
2. relative uncertainties = +/- 7% of the calculated values from 30% to 60% of the rated; power;
3. relative uncertainties = +/- 20% of the calculated values below 30% of the rated power.

Another key point for the assessment of the uncertainties of PV+WT generation is the interannual variability of the sources, as already discussed.

D. Investment and Operation under RES Uncertainty

In evaluating the pathway towards decarbonized electricity systems, the generation potential from the RES such as solar and wind are used in optimization models for the planning and operation of the electricity system. Most studies with a focus on RES integration rely on single-year RES data. Such analyses, although they provide optimal solutions for the studied year's data, are not comprehensive due to spatial-temporal variations of RES over longer periods of time.

Year-to-year variability of renewable resources can substantially change the optimal capacity investment and its operation in different years, leading to inaccurate economic evaluations. Relying on single-year data of RES for investment decisions can result in flexibility, reliability, and financial issues for the system. A system that is optimized for one year of RES may face capacity inadequacy in other years, which may cause load curtailments and lower reliability. Higher load curtailments also lead to high operational system costs, which could be prevented by appropriately accounting for the RES variability. In addition, insufficient investment in flexible resources such as energy storage may increase RES curtailment leading to waste of clean energy resources.

Therefore, there are several key challenges in power systems planning and operation problems with high shares of RES, including 1) consideration of high-resolution RES generation availability data for multiple years, 2) accounting for RES forecast uncertainty in operating reserve requirements and system dispatch, 3) adequately representing flexibility characteristics of generation, demand, and energy storage [47]. To address these challenges, the objective function of a stochastic generation expansion problem can be expressed as in (9):

$$\min C = \sum_{g} \left(C_g^{Inv.} \times A_g + C_g^{FixOM} \right) \times \delta_g^{Inv.}$$

$$+ \sum_{s} \left(C_s^{Inv.kW} \times A_s \times \delta_s^{Inv.kW} + C_s^{Inv.kWh} \times A_s \times \delta_s^{Inv.kWh} + C_s^{FixOM} \times \delta_s^{Inv.kW} \right)$$

$$+ \sum_{y} \left[W_y \left(\sum_{t} \left\{ \begin{array}{l} \sum_{g} C_g^{VarOM} \times \phi_{g,y,t} + \\ \left(C_s^{VarOM} \times \phi_{s,y,t} \right) + \left(C^{ENS} \times \gamma_{y,t}^{e} \right) \end{array} \right\} \right) \right]$$

(9)

The objective is to minimize the investment and operation costs of the system considering multi-year variations of the RES and load. $C_g^{Inv.}$ is the investment cost of generation technology g (\$/MW), A_g is its annuity factor and $\delta_g^{Inv.}$ is its invested capacity (MW). C_g^{FixOM} is the annual fixed O&M cost of generation technology g in \$/MW-yr. $\delta_g^{Inv.}$ is the total installed capacity of g in the target year. Similarly, for the storage technology s, investment in the power and energy components and the fixed O&M costs are included in the objective function. Note that the Energy Storage System (ESS) power ($\delta_s^{Inv.kW}$) and energy ($\delta_s^{Inv.kWh}$) capacities are optimized separately. W_y is the weight used to normalize the costs to an annual value for year y. C_g^{VarOM} and C_g^{Fuel} are the variable O&M and fuel costs of generation technology g and ϕ_g is the energy injected into the system by g. C_s^{VarOM} and $\phi_{s,t}$ are the variable O&M cost and charged/discharged energy to/from the ESS. C^{ENS} is the cost of Energy Not Served (ENS) (demand curtailment) and γ_t^{e} is ENS (MWh) at time t. This objective function is subject to different technology-specific and system-level constraints, e.g.:

- Generation units' investment and operation constraints
- ESS cycling and degradation constraints [48]
- Grid constraints
- Export constraints
- CO_2 emissions constraints

- Hourly energy balance constraints

It is important to note that the generation from RES is primarily used to serve the local load. Additional RES resources can be exported or stored in the ESS for later use. This generic formulation can be used to evaluate the role of RES inter-annual variability and uncertainty on the optimal system configurations and propose robust solutions for the generation portfolio and its operation based on multiple years of measured or projected RES data in different locations. The RES data for different times and locations can be obtained from tools such as RES-PLAT and used as an input to generation capacity expansion planning.

E. Architecture of the platform

The "RES-Plat" platform has been designed to analyze, in an integrated way and from an energy planning perspective, the multi-dimensional impacts of the exploitation of renewable energy sources (RES), with particular reference to wind and photovoltaic [49].

The platform is based on a proprietary database, implemented in PostgreSQL, powered by different publicly available datasets (namely, PVGIS, SoDa, MERRA-2, OpenStreetMap, GHS-POP, NaturalEarth, Copernicus, Sentinel Hub), from which quantitative information relating to different parameters are extracted. The considered parameters are: global radiation (measured in kW/m^2, it is the main input for assessing the power and energy production of PV systems; hourly data are collected from 2012 to 2016 on 4 mounting types); air temperature (measured in °C, it allows to define PV cell operating temperature and air density variation, which affects the electricity generation from wind turbines), wind speed (measured in m/s, it is the main parameter for the calculation of power and energy production of wind turbines, and it is used to increase the accuracy of PV production models; altitude (measured in m, it includes both the average and the maximum values for evaluating the shading effect of mountains and hills; it is also used to obtain the mean slope (%), surface typology (it affects the RES plant installations; it includes information on buildings (surface), land cover (water and forest), presence of desert areas and population (cities with more than 50000 inhabitants)); terrain roughness (measured in m, it represents the height variation of terrain affecting, according to a logarithmic law, the wind speed).

An interactive cartographic representation allows users to automatically identify the areas suitable for plant installation based on the above-mentioned physical, environmental and topological parameters and proper inclusion/exclusion criteria and thresholds set by the analyst. From the spatial point of view, the analyses can be carried out at different administrative levels (countries, regions, districts, or single points). The cartographic data are processed by resampling on square cells with a 10 km side. This grid represents the most refined level of spatial granularity: however, the information is visualized by the users as a single datum, corresponding to the centroid of the cell. The data are further re-aggregated (as average values) on the three administrative entities (districts, regions, countries) that constitute the upper levels of granularity. The current geographical coverage includes 32

countries of the Mediterranean area, even if further expansions are planned and ongoing. Figure 11 shows an example of the geo-referred mapping of solar irradiance in the "RES-Plat" platform.
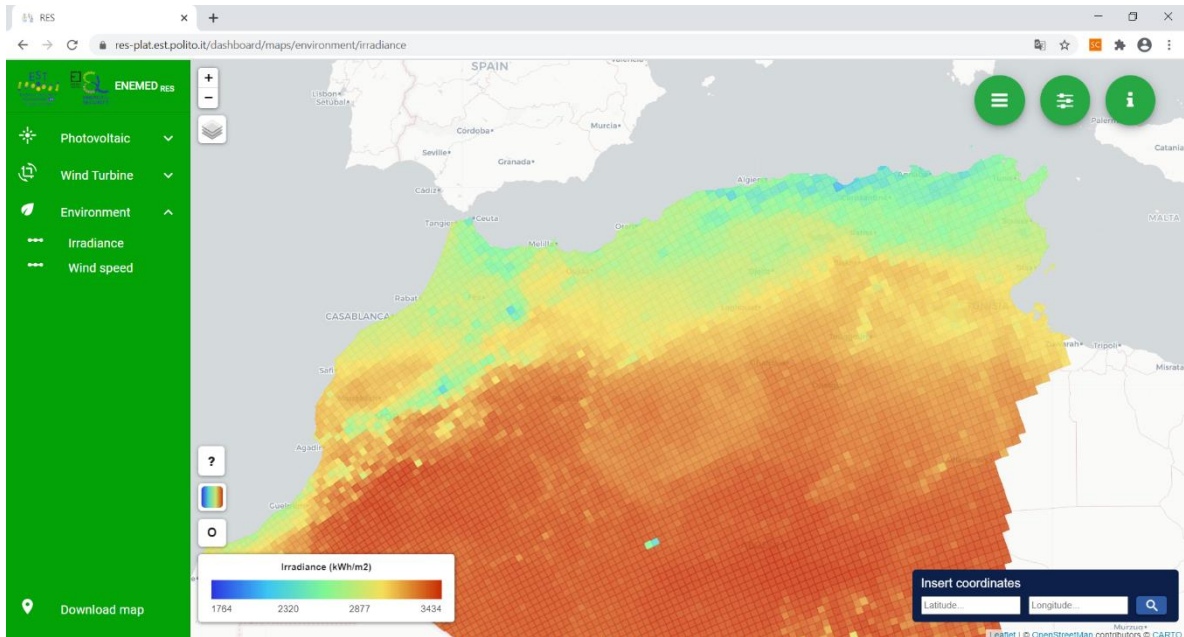

Fig. 11.   Example of georeferred mapping of solar irradiance in the "RES-Plat" PLATFORM

The user can create simulation cases by selecting the location of interest on the map, choosing a technological option among 4 PV mounting types and 3 wind turbines (with different performance levels), setting the simulation parameters, and activating the calculation kernel (developed in Python language) for the execution of the run. Through proper function libraries, implementing the methodological approach described in this paper, and the related algorithms, the electricity production is assessed according to different time granularities (annual, monthly, hourly). Moreover, it is possible to include in the simulation and evaluation of the financial impacts of the investment (based on different metrics, like the internal rate of return, the payback time, and the net present value) and of environmental impacts (in terms of avoided CO_2 emissions).

The web interface is organized into a backend section (based on Django-REST framework) and a frontend section (based on the modular JavaScript library React). The interactive mapping is instead based on the JavaScript library Leaflet. For the related web server, the Python Web Server Gateway Interface (WSGI) HTTP server Gunicorn and the webserver/reverse proxy NGINX are adopted.

The obtained results can be exported in the form of data tables, maps, and computational narratives (based on the interactive computational platform Jupyter Notebooks; this last typology of output is presently under development).

A schematic representation of the conceptual platform architecture is shown in Figure 12.
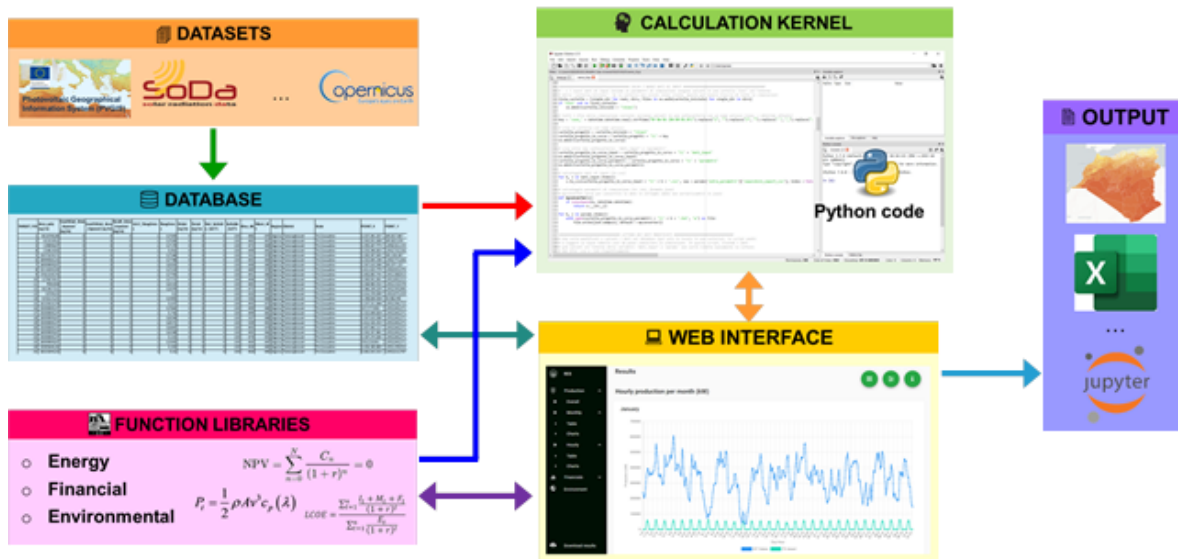
Fig. 12. Conceptual architecture of the "RES-Plat" PLATFORM

In the framework of a close synergy between data management, georeferenced mapping, and implementation of mathematical models, the strong interaction between the visualization part, constituted by the GIS (Geographic Information System) representation and the analytic part, represented by the automatic pre-screening of the considered territory in terms of suitability of a given site according to the type of technology to be installed, constitutes one of the main and novel features of the tool. In fact, unlike the analysis platforms that integrate geo-referenced representation modules and that are usually based on atmospheric data (as solar irradiance and wind speed), acquired through remote sensing systems, like the PVGIS software of the European Commission [11] and the "Global Wind Atlas" (developed by the World Bank and the Technical University of Denmark) [50], the "RES-Plat" platform integrates additional advanced topographic data (like the previously mentioned urbanization, terrain roughness, desert surface) with a homogeneous coverage. This makes the platform a planning tool able to perform simulations coherent with the optimal and rational exploitation of the territories.

IV. CASE STUDY: RES EXPLOITATION IN EGYPT

In this chapter, the procedure for planning purposes in terms of energy figures is presented with respect to a real case study. After the implementation of the models described in Section III, temporal and geographical variations in productivity are studied for both PV plants and wind farms. After that, the procedure continues with the analysis of the profiles for the different seasons and the study of the contemporaneity of the two sources.

It is worth noting that the presented procedure has the ability to plan both the installation of a new PV+WT generation and the upgrading of a remarkable PV+WT portfolio in a developed country.

Indeed, as an example of this second application, the expansion from the current 25% (about 20% from WT and 5% from PV) of the consumption to more than 50 % of the consumption might be planned in Spain. In this country, the national load profiles are well-known on an

hourly basis (from the Spanish TSO Red Eléctrica [51]), and the High Voltage (HV) transmission grid is highly meshed.

In this way, it is realistic to assume that the probability of congestions on the HV lines is negligible in case of substantial power injection from multiple sites. The windy and sunny sites are chosen with the constraint to be near the main cities for minimizing the transmission and distribution losses. This guess justifies the omission of the power flow calculations that would require the knowledge of the electrical parameters for the transmission-grid lines: these data are not available in the majority of the real cases.

Following these assumptions, from now on, the planning of PV+WT generation is carried out in the principal urban areas of a developing country, where the transmission lines are already sufficiently meshed, as for example Egypt, that has a population double with respect to Spain and about 25 % of the Spain GDP.

The selected 6 urban areas include multimillion population with the current availability of electricity for the most of time. The profiles of load consumption are derived from the Spanish profiles applying a scale factor, taking into account the corresponding national consumption on a yearly basis.

A. Selection of suitable sites for RES in <u>Egypt</u>

Egypt is an interesting case study for the analysis of the renewables potential due to different favorable conditions. Egypt has an area of 1,001,000 km^2 and is one of the most populated countries in Africa and the Middle East, with a density of 100 ab/km^2. Most of its 100 million inhabitants live along the banks of the Nile River, where the country's only habitable land is located [52]. Excluding sandy desert areas, in the other parts of the country, there are wide areas not suitable for farming but adequate for the installation of PV and WT technologies. The high number of inhabitants leads to the highest consumption and generation profiles in Northern Africa [52], with the real possibility of reaching high self-sufficiency from renewables.

With regard to renewable sources, it is a country with high solar radiation intensity, varying annually between 2000-3000 kWh/m^2 (with single-axis tracking), and it is characterized by very favorable windy conditions, especially along the banks of the Nile River and along the Suez Canal.

In conclusion, in the next decades, Egypt will play a crucial role in the future synergic development between Africa and Europe, in the framework of a new, integrated Mediterranean energy system based on renewables [53].

The search for the locations was carried out following the criteria described in Section III and leading in the selection of six representative sites. These sites are close to the capital Cairo and the cities/towns Matruh, Ras Gharib, Hurghada, Luxor, and Aswan and satisfy the constraints for the development of RES. Some details about the selected sites are described below.

Site #1 is located between Alessandria and Marsa Matruh, which is one of Egypt's most important ports overlooking the Mediterranean. It is served by a 220 kV transmission line and will be served by a 500 kV line, currently under construction [54]. It has favorable conditions for wind and solar sources. Being close to important population centers (Alexandria has more than 5 million (M) inhabitants), this site allows for local self-consumption.

Site #2 is an area close to Ras Gharib, which is located along the shores of the Gulf of Suez. Ras Gharib is a small town (0.3 M inhabitants), but it is Egypt's second most important oil loading port and trading area. Two transmission lines of 220 kV and 500 kV are under construction to better connect this area to the electric grid [54].

Hurghada is the location chosen for site #3, and it is along the Gulf of Suez. It is one of the most important tourist destinations in the Red Sea, near Hurghada International Airport. It is a small town (100k inhabitants) with important commercial touristic activities. The area is served by a 220 kV transmission line [54]. Confirming that they are favorable areas for the installation of photovoltaic and wind systems, there are already important projects under development.
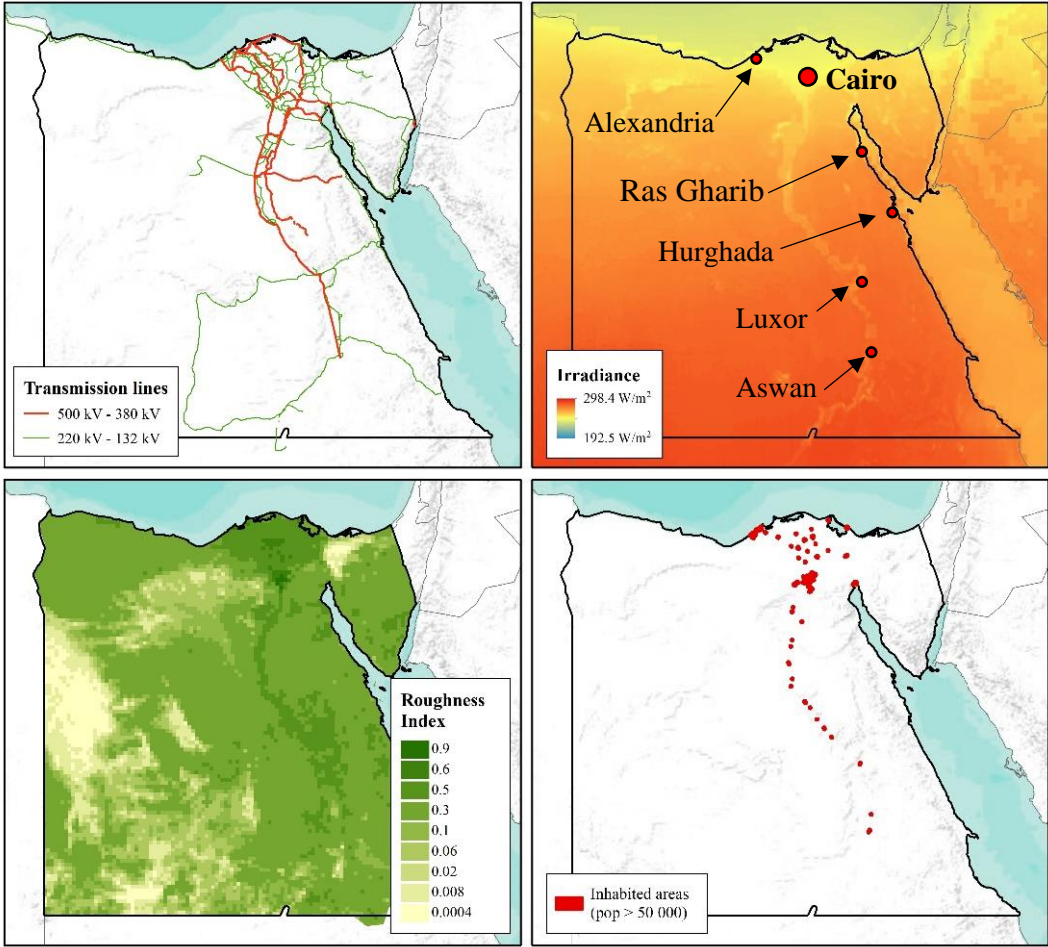

Fig. 13. Top-left: the red and green lines represents the HV lines already working. Top-right: map of mean solar irradiance. (Bottom-left) roughness index of the terrain. (Bottom-right) biggest inhabited areas

A 2 GW wind farm is planned along the Suez Canal, while a 20 MW PV plant is being developed in the vicinity of Hurghada. At the present time, there are a total of 11 wind and 10 scheduled photovoltaic plants for a total size of 7 GW [53].

Site #4 is close to Luxor (1.3M inhabitants), which is an important center both from an archaeological and tourist point of view, in the vicinity of which there is also Luxor international airport. The area is served by transmission power lines of 132-150 kV, 220 kV, and 500 kV. Near the chosen area, there are several other inhabited centers, permitting local self-consumption.

Site #5 is close to Aswan, which is a large city with about 1.6 M inhabitants, located on the east bank of the Nile, and it is a tourist and commercial center. The area is served by transmission power lines of 132-150 kV, 220 kV, and 500 kV [54].

Figure 13 shows the six sites on different maps related to some of the criteria used for the selection. In each of the above-described locations, the land is arid but a non-sandy desert area. The terrain is mainly flat and rocky; thus, it is not suitable for farming. There are wide areas with no architectural, naturalistic, military, or other particular restrictions for the installation of utility-scale PV systems and wind farms. From the technological point of view, the PV generators have sun-tracking systems (single or double axis) to follow the apparent path of the Sun: this permits a yearly increase of production of >30% with respect to fixed systems and lower seasonal variations. Thanks to the increase in efficiency and even lower costs, these systems are supposed to gain market share.

Finally, the last site (Site #6) is the metropolitan area of Cairo with a population of about 20 M. In this case, it is considered the installation of small PV generators on the rooftops of the buildings; no wind turbines are considered in this area due to the high population density.

B. RES productivity in Egypt

Figure 14 shows yearly PV and WT estimated energy productions in Site #1 from 2005 to 2016. Energy productions are calculated following the models described in Section II, subparagraph B, and refer to plants with a nominal power of 1 MW. The irradiance and air temperature inputs profiles have 1-h time step, and are obtained from [11].

The PV production is almost constant: over the 12-years, the average is 2682 MWh/MW$_p$. The standard deviation is 59 MWh/MW$_p$, corresponding to 2.3% of the average. On the contrary, the annual variation of wind power production is not negligible: the average is 3103 MWh/MW with a standard deviation of 488 MWh/MW (about 16% of the average). In fact, in the year 2009, the estimated wind production is minimum (2466 MWh/MW), while it is maximum one year later (3651 MWh/MW). These variations are related to the difference in the wind speed at 10 m height: the annual average was 3.7 m/s in 2009, and it increased up to 4.5 m/s in 2010.

The calculations refer to new installations without considering the performance degradation of the plants [44]. Table VI presents the productivities for PV and wind power systems in the six sites under analysis; their standard deviations are calculated in 2005-2016. As previously

mentioned, the PV productivity refers to generators with an inclined axis, while in Cairo it is indicated the productivity of building-integrated PV systems.
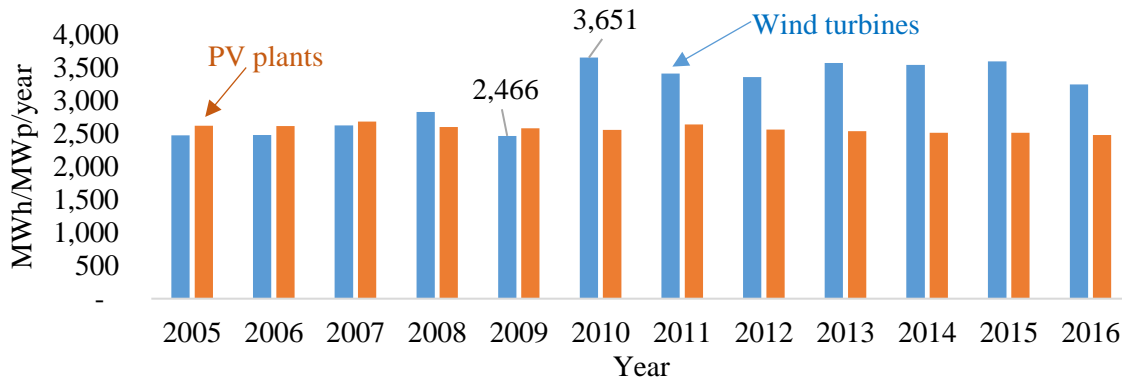

Fig. 14.   Hearly Productivites for PV generators and Wind Farms Installed in Site #1

TABLE VI. WIND AND PV PRODUCTIVITY IN EGYPT

Yearly productivity of PV and wind systems			
Mean value ± st. deviation (MWh/MW/year)			
Site #	*Nearby city/town*	*PV systems*	*Wind farms*
1	Alexandria	2446 ± 4.1%	3016 ± 8.3%
2	Ras Gharib	2631 ± 3.9%	2554 ± 13.5%
3	Hurghada	2626 ± 3.8%	5080 ± 13.9%
4	Luxor	2555 ± 2.9%	3693 ± 8.6%
5	Answan	2546 ± 2.3%	2870 ± 15.7%
6	Cairo metropolis	1840 ± 3.0%	-

The PV productivity is geographically and temporally homogeneous. In particular, PV production varies between ≈2300 MWh/MW near Alexandria up to a maximum of ≈2600 MWh/MW near Luxor. On the contrary, the productivity of wind farms is much more different site by site and having a higher interannual variability than in the case of PV systems. The WT power production varies from ≈2500 MWh/MW near Alexandria to a maximum of 5083 MWh/MW near Hurghada, which is the windiest site.

It is noted that thanks to the geographical location, the favorable weather conditions, and the use of PV plants with the tracking system, there is relatively constant PV production on a monthly basis. Considering the years 2006-2015, the monthly PV production is about 1.08±5% TWh in February, 1.41 ± 2% TWh in June, and 1.30 ± 2% TWh in September. As a result, the relative variation between the minimum and maximum monthly production is in the range 20÷30% for PV. In the case of wind farms, this ratio is in the range 40÷60%.

Figure 15 and Figure 16 show examples of hourly production profiles for PV generators and wind farms installed in all the analyzed sites for the months of February and July, respectively. They are calculated considering an installed power of 1 GW per each technology and each location (6 GW of PV plants and 5 GW of wind farms). These examples well represent the general situation: the absence of PV production during night hours is

partially compensated by the presence of wind source in every period of the year. It is confirmed in Figure 17, where the production of the year 2016 is referred to as the nominal power and sorted from the smallest to largest. In this way, it is possible to compare the production of only wind turbines, only PV systems, and a portfolio including both technologies. As a result, the use of PV+WT almost halves the number of hours in which the generation is below 20% of nominal power, with respect to the use of only PV systems.
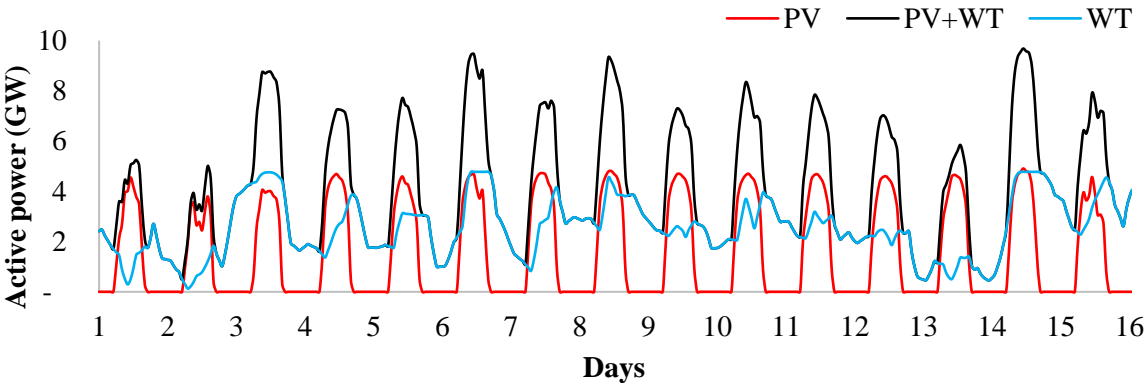

Fig. 15.   Example of hourly cumulative production profiles for PV generators and wind farms installed in all the analyzed sites in Egypt – February 2016
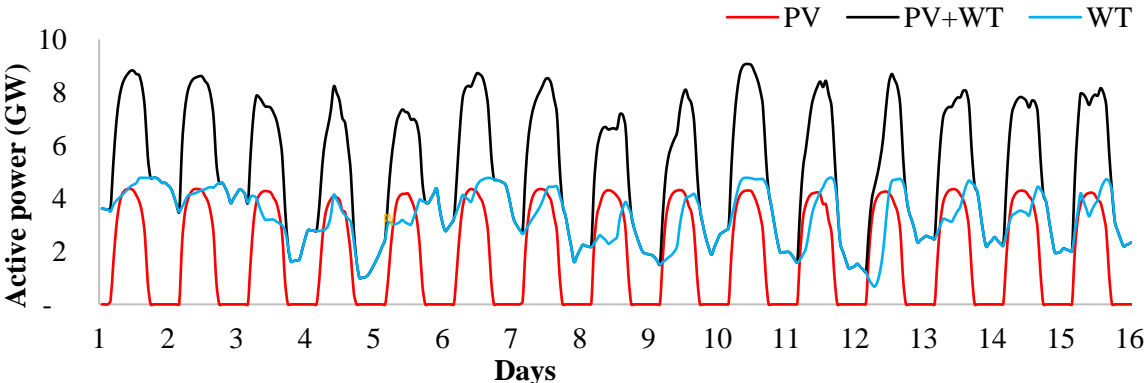

Fig. 16.   Example of hourly production profiles for PV generators and wind farms installed in all the analyzed sites in Egypt – June 2016
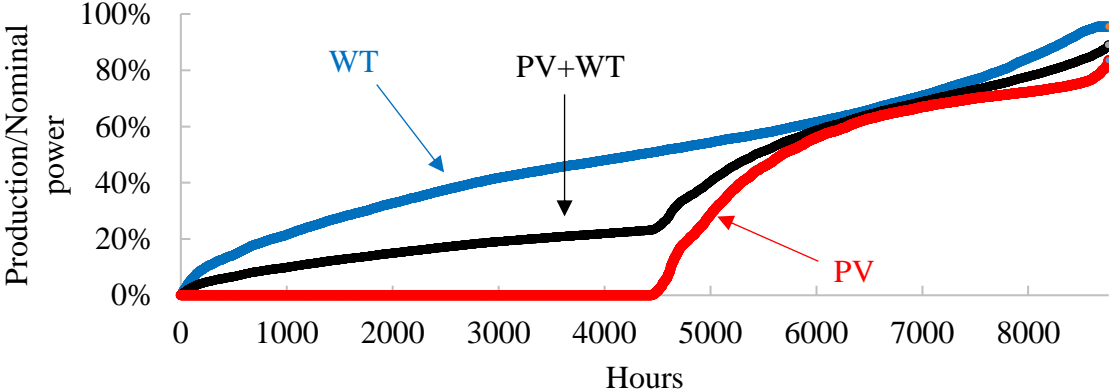
C. A Possible Electricity Trade Between Africa And Europe: the role of Egypt

High penetration of renewables in the power generation system of North African countries, allowing them to fulfill their internal demand completely, could permit the generation of a surplus, which could be used for building a new energy dialogue and exchange based on RES between the southern and the northern shore of the Mediterranean sea (i.e., with European countries). According to this, a scenario analysis up to 2040 has been performed, with reference to Egypt, to quantitatively assess the possibility of RES exploitation in terms of annual energy production and hourly power injection through the methodology originally developed and described in Section III. The focus of the analysis has been on WTs and solar PV, which – among the different renewable sources – currently seem to be the most promising options, although concentrated solar, wave, and geothermal energy might play a role in the future [52].

D. Productivity scenarios

The energy production profiles from PV and wind power installations are obtained by means of the "RES-Plat" platform. For the case study, several locations of Egypt were selected based on the criteria described in Section III. In particular, the database provides hourly values of weather data (irradiance, air temperature, and wind speed) from 2006 to 2016. Regarding future production, three scenarios are considered:

- *RES low:* power generation from RES is used only for fulfilling the electricity demand of Egypt;
- *RES medium*: besides the fulfillment of Egypt electricity needs, a surplus can be available for trans-Mediterranean exchanges, depending on the considered load scenarios;
- *RES high*: significant electricity surplus is available for exchanges between Egypt and European countries.

E. Demand scenarios

Currently (2017 data), the electricity production of Egypt is equal to 185 TWh, while the electrification of the final energy consumption corresponds to 22.7%, and it is particularly high in the residential sector (41.8%), and in the commerce and services sector (100%), while in the industry it reaches 23.6% and it is almost negligible in transport (0.2%) [55].

Regarding the projections of the Total Final Energy Consumption (TFC) and of the related electrification rate by 2040, two scenarios are considered:

Reference scenario: the TFC and the electricity consumption are projected to 2040 on the basis of the best fit of historical data. In particular, the time horizon 1971-2017 has been considered. Regarding the TFC projections, good fittings have been obtained by means of linear trend, with a coefficient of determination R^2 equal to 0.96, while for electricity

consumption the historical data can be best fitted by a logarithmic trendline, with R^2 equal to 0.92.

This leads to an overall increase of the TFC equal to 37.7% over the period 2017-2040, corresponding to an average annual growth rate of 1.4%.

- *High Electrification scenario:* it has the same projection approach as the Reference scenario for TFC, while the electrification rate is assumed to reach 50% by 2040. According to this, the electricity consumption in 2040 has been calculated as half of the projected TFC in the same year, assuming a linear growth between 2017 and 2040.

Table VII summarizes the scenario projections in terms of the TFC and electrification ratio.

TABLE VII. SCENARIO PROJECTION UP TO 2040 FOR EGYPT

Scenario projections				
Scenario		**2017**	**2020**	**2040**
Scenario 1 - Reference	TFC [TWh]	707.8	742.6	974.5
	Electrification [%]	22.5	22.5	22.2
Scenario 2 - High electrification	TFC [TWh]	707.8	742.6	974.5
	Electrification [%]	22.5	27.2	50.0

F. Overall scenarios

Three overall scenarios have been built by combining the production and consumption scenarios previously described:

1) Scenario A: RES low + Reference
2) Scenario B: RES medium + Reference
3) Scenario C: RES medium + High electrification
4) Scenario D: RES high + High electrification

The main energy results in terms of production, load, and surplus of the three scenarios in 2040 are summarized in Table VIII.

TABLE VIII. SCENARIOS PROJECTIONS IN 2040 FOR EGYPT

Scenario	Electricity [TWh/y]		
	Production from RES	**Load**	**Surplus**
A	216	216	0
B	293	216	77
C	490	490	0
D	681	487	194

In Scenario A, the installed power of PV and WT is in the range 78-87 GW; these resources fully supply the yearly electric loads of Egypt, corresponding to 216 TWh in 2040. In Scenario B, the higher installed capacity (106–117 GW) allows Egypt to produce a significant annual surplus in 2040 (77 TWh), available for trade with other countries and corresponding

to 26.3% of the Egyptian electricity generation. In Scenario C, PV and WT total installed power is in the range 140-170 GW; these resources fully supply (on a yearly basis) the electric loads of Egypt in the high electrification scenario, corresponding to 490 TWh in 2040. Finally, in Scenario D, the installed power of PV and wind system (245–270 GW) totally supply the electric load (corresponding to an electrification rate of 50%, according to the scenario hypothesis) and ensure a surplus of about 194 TWh for trade with foreign countries.

G. An Electricity Trade Scenario Between Egypt And Europe

The energy surplus that can be generated in North Africa requires an adequate development of infrastructures to transfer it to the other countries and, in particular, towards Europe. Currently, ten electricity interconnections across the Mediterranean are in operation, with an overall capacity of about 5 GW. However, significant investments are already ongoing or planned: 3 new interconnectors are under construction, 9 are in the permitting phase, 1 is planned, and 7 are under consideration, corresponding to a possible total increase up to about 21 GW. The total investments for these infrastructures can be quantified to 21 billion € [56]. Despite the huge investments, there could still be a bottleneck effect due to the transmission lines between North Africa and Europe with reference to the exploitation of the possible generated surplus of electricity from RES in North African countries. In fact, a reasonable capacity of 12.5 GW for the interconnectors linking Europe and North Africa in 2040 can be expected.

Focusing on Egypt, in particular, two main infrastructures will connect it with European countries: the EuroAfrica Interconnector, from Egypt to Greece, with a capacity of 2 GW and an overall length of 1545 km, and the TREY, from Turkey to Egypt, with a capacity of 3 GW and a length of 700 km.

Theoretically, considering an overall transmission capacity of about 5 GW between Egypt and the EU, the yearly maximum exportable surplus could be 43.8 TWh/year. Table VII shows that according to the simulations carried out in the case study, in Scenario B, only 16.6% and in Scenario D, only 6.8% of the total available annual electricity surplus from Egypt in 2040 could be exported to Europe, mainly due to the limited overall capacity of the hypothesized infrastructures.

Nevertheless, from a market perspective, the import of electricity from RES could lead to a reduction in European electricity prices, thus resulting in economic savings and therefore creating a positive impact for both the areas, underlining how further efforts in creating electricity interconnections across the Mediterranean Sea could be a valuable option for facing, in a more cooperative way, the multifaceted challenges related to the energy transition [53].

TABLE IX.   ELECTRICITY EXPORT FROM EGYPT TO EUROPE BY SCENARIOS IN 2040

[TWh/y]	**Annual electrical energies [TWh]**			
Scenario	**A**	**B**	**C**	**D**
Available RES surplus	0	77	0	194

[TWh/y]	Annual electrical energies [TWh]			
Scenario	A	B	C	D
Export from Egypt	0	12.8	0	13.1

As an additional consideration, this new energy dialogue between the two shores of the Mediterranean Sea can be further strengthened if a wider energy interplay strategy involving electricity, hydrogen and gas is considered. In fact, since the increasing exploitation of RES has to be coupled with an increase in the storage capability of the energy systems. Among storage technologies, the Power-to-Gas (PtG) can play a crucial role in the area. From one side, starting from electricity generated from RES, it allows to produce "green" hydrogen (through electrolysis) and Synthetic Natural Gas (SNG, through methanation). In particular, hydrogen could be particularly helpful for achieving, in the long run, a carbon neutrality condition, allowing for the decarbonisation of sectors that cannot be decarbonized through the use of electrical technologies (e.g. the production of high temperature heat for industrial processes), and that – at European level – is expected to play a major role in the framework of the "Next Generation EU" recovery plan; with reference to this, the EU "Hydrogen Strategy" [57] already forecasted an hydrogen penetration by 2050 able to cover a share of the final energy uses ranging between 13% and 23%. From the other side, this energy interplay among these three commodities creates a link also among the main energy infrastructures, namely gas pipelines and electricity network, which respectively presently play and are expected to play in the future a key role in the energy exchange in the region. In particular, the production of both hydrogen and SNG could allow a higher exploitation of the existing gas pipelines, whose capacity is currently not completely used; the utilization of gas pipelines could ensure an easy energy storage for long time, without requiring a "just-in-time" balancing between generation and load (like for electricity). Of course, ad hoc analyses for deeply exploring the pros and cons of this option have to be performed, especially with reference to the overall system efficiency.

H. Optimal Investment and Operation under RES Uncertainty

To show the impact of RES data variability on the optimal investment and operation, we use 10 years of weather data and the projected load data for 2040. Table X shows the assumption for this analysis, based in part on [58][59][60]. We evaluate the investment in PV, wind, and ESS in four scenarios of (a) availability of 50 GW existing grid capacity in Egypt (mainly gas-powered plants), (b) no existing grid capacity, (c) 50 GW grid capacity with 5 GW export capacity and (d) 50 GW grid capacity with 12.5 GW export capacity. Investments in PV and wind capacities are constrained to the projected maximum values. The grid and the export capacities are assumed to be firm; however, the hourly dispatch is optimized.

TABLE X. INPUTS AND ASSUMPTIONS FOR SYSTEM IN 2040

	PARAMETER	VALUE
PV	Investment cost ($/kW)	628

	Projected Max capacity (GW)	99
Wind	Investment cost ($/kW)	1222
	Projected max capacity (GW)	55
Storage	Power component investment ($/kW)	300
	Energy component investment ($/kWh)	100
	Charge/Discharge efficiency	0.9
	Cycle/Calendar life (cycles/years)	6000/20
Grid	Firm capacity (GW)	50
	Energy cost ($/MWh)	73
Export	Max tie-lines capacity (GW)	5 or 12.5
	Energy revenue ($/MWh)	200
Load	Annual sum (TWh)	490

Figure 18 shows the optimal capacities, ESS duration, and the energy cost for scenarios (a) and (b). Based on these results, with 50 GW grid availability, the optimal solution includes the maximum available wind capacity (55 GW), while PV's optimal capacity varies between 61 GW and 82 GW depending on the weather year. On average, 20 GW of ESS capacity is also required in this scenario. In scenario A), the ESS energy component is 9 hours duration on average. Generation from the grid also provides flexibility to integrate RES in this case. The energy cost per is 48 $/MWh in this scenario which includes capital and operation costs. However, without existing grid capacity in scenario B), investment in both PV and wind reaches their maximum limits, and 78 GW of ESS capacity is built on average. In this scenario, due to variations in the weather data in different years, investment in ESS has high variations across the years, and the system requires substantially longer ESS durations. High investments in ESS do not prevent capacity inadequacy in this scenario, and there are substantial load curtailments in the optimal solution (10% of the total load) which is reflected in much higher energy cost per MWh.

a: PV + Wind + ESS + 50GW grid capacity   b: PV + Wind + ESS (0GW grid capacity)
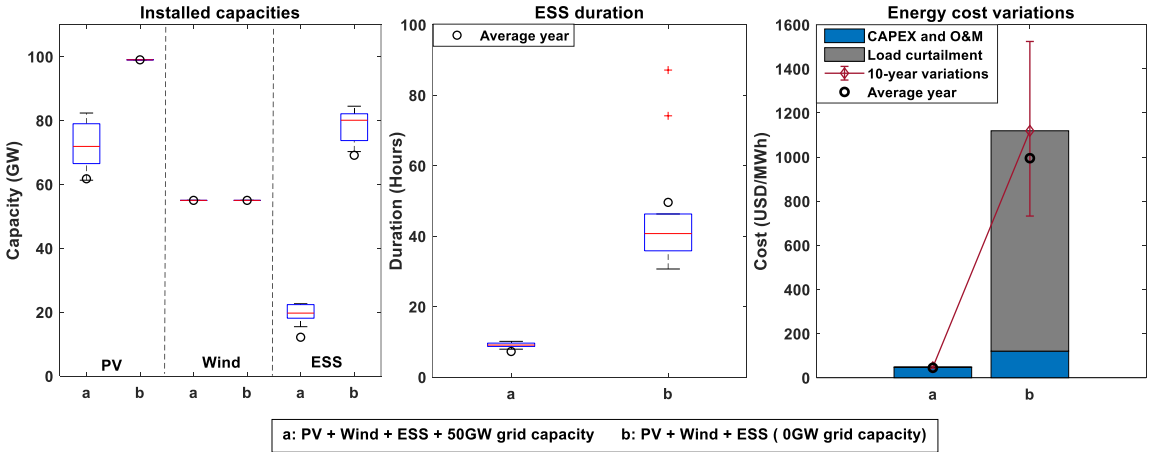
Fig. 18.   RES and ESS optimal investment and system's operation in 2040 for 10 years of historical weather data

In scenarios (c) and (d), we investigate the potential for electricity export from Egypt to Europe. Table XI indicates that the total system cost increases with export due to the larger investments in PV and increased generation from the existing grid. However, the revenue

from electricity export to Europe compensates for the increased system costs. In this case, the grid electricity is used to serve the local load, and the PV and wind generations are exported. Note that the wind and ESS capacities do not change substantially with export. With the assumption of constant average emissions for the local grid electricity, increased dispatch of the local grid increases the CO_2 emissions substantially. It is important to mention that all these results should be interpreted according to the assumptions used in this study.

TABLE XI. OPTIMAL ELECTRICITY EXPORT IN 2040 FOR DIFFERENT EXPORT CAPACITIES

	No export	(c) 5 GW export capacity	(d) 12.5 GW export capacity
Total system cost (billion $)	22.1	24.5	27.9
CO_2 emissions (million tons)	68	81	99
Export revenue (billion $)	-	8.7	21.6
PV Export (TWh)	-	14.6	25.2
Wind export (TWh)	-	29.1	82.8
Total export (TWh)	-	43.7	108.0
PV optimal capacity (GW)	61.7	69.4	81.7
Wind optimal capacity (GW)	55.0	55.00	55.0
ESS (GW/GWh)	12 / 88	12 / 89	12 / 89
Load curtailment (MWh)	4942.5	4199.6	4199.6

Focusing on the EES, the adopted model takes into consideration electrochemical storage systems, according to their current techno-economic characteristics. However, it has to be highlighted that the implemented storage model is an energy model, i.e. based on energy and economic inputs (like charge/discharge efficiency, life, investment cost) and independent from the considered storage technology (e.g. Lithium or lead-acid batteries). The adopted model is able to manage different storage types, and it could be therefore easily updated on the basis of further information about technological evolution of the present electrochemical EES (mainly driven by the applications in transport sector) and used for simulating new technological options. In particular, one of the advantages of the adopted approach is the possibility to use it also for other storage technologies, like the hydroelectric pumped storage [62], particularly relevant in developing countries, especially coupled with photovoltaic power generation. This option could be modelled similarly to the electrochemical storage, where the state of charge corresponds to the level of water and the charge/discharge efficiencies are equivalent to the efficiencies of the pumping phase and of the turbine.

V. CONCLUSIONS

This paper presents an interdisciplinary procedure suitable for the planning of RES, with a focus on photovoltaic and wind generation. In fact, electricity, as the most direct and effective use of RES, is the center of the energy transition. The procedure is built not only for research purposes but for all the stakeholders involved in the transition to renewables. The procedure defines the key points for the assessment of large-scale RES installation and presents a

platform useful to effectively analyze the massive quantity of data resulting from the simulations.

The start is the definition of the most suitable sites for RES; e.g., the most promising energy production. Besides the weather data analysis, the study of terrain morphology is of fundamental importance for the correct forecast of energy production, such as the check of extreme weather conditions. For utility-scale installation planning, the analysis of the connection with the electric grid is fundamental, such as the check of the proximity to huge electric loads to increase their self-sufficiency.

Regarding the mathematical models for the assessment of energy production, the present work compares the calculation of PV production by using two models. The SDMl is interpolated by a straightforward model including different types of losses in the energy conversion. As a result, the straightforward model is always conservative with respect to the SDM, and the annual energy deviation is acceptable, because it is within the uncertainty of instruments for measurement of weather data. A similar comparison is performed for three types of wind turbines in different sites. The results show that the type with the biggest rotor and greatest height has a productivity up to ≈+40% with respect to other models for the good exploitation of low wind speed, but also higher maintenance costs due to greater wear.

RES by itself is not the only aspect to be considered in the energy transition; RES should be fit together with the development of transmission infrastructure, electrification of the final uses, and the support of storage systems. In order to consider all these aspects, the procedure takes into account interannual variability and uncertainty of RES in the system planning and operation problem using multiple years of RES data: the goal is to find optimal solutions for the generation system configuration, which has to be robust over the years with high differences in weather conditions.

The case study on the RES exploitation in Egypt, using the prototype web-based platform "RES-PLAT" at EST@ Energy Center – PoliTO lab, shows the presence of large areas suitable for the development of utility-scale RES plants. As a result of the analysis of 10 years with 1-hour step, the PV productivity (inclined axis systems) is geographically and temporally homogeneous: it varies in the range ≈2300÷2600 MWh/MW in the whole country. On the contrary, the WT power production is geographically and temporally more variable, and it is in the range ≈2500÷5100 MWh/MW. The combination of the two technologies almost halves the number of hours in which the generation is below 20% of nominal power, with respect to the use of only PV systems.

According to these production data and the other assumption considered in different generation and load scenarios, the impact of RES data variability on the optimal investment and operation is evaluated. The high potential of PV and wind turbines in Egypt can easily fulfill the internal yearly electricity demand even in high electrification rates, making it possible to also trade with Europe. To satisfy the yearly electrical load in high electrification, PV and WT total installed power should be in the range ≈140-170 GW, while a considerable surplus available for Europe is possible installing ≈245–270 GW.

If PV and WT are sized only to meet the annual internal demand (140÷170 GW), there is not always a perfect match between generation and load on an hourly basis: other sources, storage systems, and imports are necessary to feed loads; otherwise, load curtailment would be necessary. Simulation results show that in the case of 5 GW of interconnection with EU and a grid capacity of 50 GW (mainly from natural gas) lead to the necessity of a storage capacity of ≈20 GW. This storage capacity supports the optimal sizes of PV and wind in the worst weather years (82 and 55 GW, respectively).

Finally, the results of the case study show that total system cost increases with export due to the larger investments in PV and increased generation from the existing grid, but the revenue from electricity export to Europe compensates for the increased system costs. Moving from an expected EU-Egypt interconnection capacity of 5 GW in the year 2050 to a theoretical value of 12.5 GW, the total system cost increased with export due to the larger investments in PV and increased generation from the existing grid. However, the revenue from electricity export to Europe (mainly due to a higher optimal PV capacity that well matches the daily load variation) compensates for the increased system costs.

LIST OF *ACRONYMS*

CSP   concentrated solar power
ENS   Energy Not Served
ESS   Energy Storage System
FCR   Frequency Restoration Reserve
GDP   Gross Domestic Product
GHG   global greenhouse gas
GIS   Geographic Information System
HV   High Voltage
HVAC   high voltage alternating current
HVDC   high voltage direct current
O&M   Operation and maintenance
PV   Photovoltaic
PVGIS   Photovoltaic Geographical Information System
RES   Renewable energy sources
SC   Self consumption
SDM   Single Diode Model
SS   Self sufficiency
STR   Straightforward Model
STC   Standard Test Condition
TFC   Total Final Energy Consumption
TPES   Total Primary Energy Supply
WSGI   Web Server Gateway Interface
WT   Wind Turbine
WT#1   Wind turbine typology with the best performance
WT#2   Wind turbine typology with the average performance

WT#1   Wind turbine typology with the low performance and low maintenance

<div align="center">LIST OF SYMBOLS</div>

ξ_{mix} PV losses tacking into account all the other sources (-)

$\delta_g^{Inv.}$ invested capacity (MW) of generation technology g

$\delta_g^{Inv.}$ total installed capacity (MW) of g in the target year

$\delta_s^{Inv.kW}$ power of the ESS (kW)

$\delta_s^{Inv.kWh}$ energy of the ESS (kWh)

$\phi_{s,t}$ charged/discharged energy to/from the ESS (MWh).

γ_{therm} Thermal efficiency (-)

η_{mix} PV efficiency tacking into account all the other sources of losses (-)

η_{lowG} Underperformance at low irradiance (-)

η_{STC} PV efficiency in Standard Test Condition (-)

η_{therm} Thermal efficiency of PV modules (-)

A_g annuity factor (-) of $C_g^{Inv.}$

C^{ENS} cost of energy not served

$C_g^{Inv.}$ investment cost of generation technology g ($/MW)

C_g^{FixOM} annual fixed O&M cost of generation technology g ($/MW-yr)

C_g^{VarOM} variable O&M cost of generation technology g

C_g^{Fuel} fuel costs of generation technology g

C^{ENS} cost of energy not served (demand curtailment)

C_s^{VarOM} variable O&M cost for the ESS.

g   g-th generation technology under analysis

G   Solar irradiance (kW/m^2)

G_0 Low irradiance factor (kW/m^2)

P_{el}^{WT} Electric power output of a wind turbine

$P_{\text{str\_m}}$ PV power (kW)

u_{ref} wind speed (m/s) measured at the height of the weather station z_{ref}

u_w wind speed (m/s)

z height of the wind turbine hub (m)

z_{ref} height of the weather station (m)

REFERENCES

REFERENCES

[1] E. Bompard et al., "An electricity triangle for energy transition: Application to Italy," *Appl. Energy*, 2020, doi: 10.1016/j.apenergy.2020.115525.

[2] Yunna Wu, Ting Zhang, Rui Gao, Chenghao Wu, Portfolio planning of renewable energy with energy storage technologies for different applications from electricity grid, Applied Energy, Volume 287, 2021.

[3] V. Mohagheghi, S.M. Mousavi, B. Vahdani, A new optimization model for project portfolio selection under interval-valued fuzzy environment, Arab J Sci Eng, 40 (11) (2015), pp. 3351-3361.

[4] Y. Wu, C. Xu, Y. Ke, Y. Tao, X. Li, Portfolio optimization of renewable energy projects under type-2 fuzzy environment with sustainability perspective, Comput Ind Eng, 133 (2019), pp. 69-82

[5] L. Michi, M. Migliori, A. C. Bugliari, B. Aluisio, G. M. Giannuzzi and E. M. Carlini, "Transmission network expansion planning: towards enhanced renewable integration," *2018 AEIT International Annual Conference*, Bari, 2018, pp. 1-5, doi: 10.23919/AEIT.2018.8577446.

[6] Y. Li, Y. Chi, X. Wang, X. Tian and J. Jianqing, "Practices and Challenge on Planning with Large-scale Renewable Energy Grid Integration," *2019 IEEE 3rd Conference on Energy Internet and Energy System Integration (EI2)*, Changsha, China, 2019, pp. 118-121.

[7] Y. Li, Y. Chi, X. Wang, X. Tian and J. Jianqing, "Practices and Challenge on Planning with Large-scale Renewable Energy Grid Integration," *2019 IEEE 3rd Conference on Energy Internet and Energy System Integration (EI2)*, Changsha, China, 2019, pp. 118-121.

[8] João Graça Gomes, José Medeiros Pinto, Huijin Xu, Changying Zhao, Haslenda Hashim, Modeling and planning of the electricity energy system with a high share of renewable supply for Portugal, Energy, Volume 211, 2020.

[9] H. Lund, J.Z. Thellufsen, EnergyPLAN advanced energy systems analysis computer model, Aalborg, Denmark (2018)

[10] Homer energy PRO. Available online: https://www.homerenergy.com/index.html, accessed on 27th February 2021.

[11] Photovoltaic Geographical Information System (PVGIS). Available online: https://ec.europa.eu/jrc/en/pvgis, accessed on 27th February 2021.

[12] Global solar atlas. Available online: https://globalsolaratlas.info/, accessed on 27th February 2021.

[13] Global solar atlas. Available online: https://globalsolaratlas.info/, accessed on 27th

February 2021.

[14] Wind Exchange. Available online: https://windexchange.energy.gov/, accessed on 27th February 2021.

[15]   International Energy Agency(IEA), "Climate change-The energy sector is central to efforts to combat climate change." Available online: https://www.iea.org/topics/climate-change (accessed May 06, 2020).

[16]   International Energy Agency(IEA), "IEA Statistics." https://www.iea.org/statistics/.

[17]   Intergovernmental Panel on Climate Change, Climate Change 2014 Mitigation of Climate Change. 2014.

[18]   United Nations, "Summary of the Paris Agreement," United Nations Framew. Conv. Clim. Chang., 2015.

[19]   R. Priddle, "World Energy Outlook - Special Report Energy and Air Pollution," World Energy Outlook - Spec. Rep., 2016, doi: 10.1021/ac00256a010.

[20]   BPSTATS, "BP Statistical Review of World Energy Statistical Review of World, 68th edition," 2019.

[21]   International Energy Agency(IEA), "World Energy Outlook," 2017.

[22]   Y. Y. Deng et al., "Quantifying a realistic, worldwide wind and solar electricity supply," Glob. Environ. Chang., 2015, doi: 10.1016/j.gloenvcha.2015.01.005.

[23] E. Bompard, D. Grosso, T. Huang, F. Profumo, X. Lei, and D. Li, "World decarbonization through global electricity interconnections," Energies. 2018, doi: 10.3390/en11071746.

[24] Rinne, E., Holttinen, H., Kiviluoma, J. *et al.* Effects of turbine technology and land use on wind power resource potential. *Nat Energy* **3,** 494–500 (2018).

[25] A. Ciocia, P. Di Leo, S. Fichera, F. Giordano, G. Malgaroli, and F. Spertino, "A Novel Procedure to Adjust the Equivalent Circuit Parameters of Photovoltaic Modules under Shading," Speedam 2020, doi: 10.1109/speedam48782.2020.9161878.

[26] Douglas-Westwood, "Offshore Wind Assessment in Norway". Available online: https://www.nordicenergy.org/wp-content/uploads/2012/01/nordvind_finalreport_16_11_2010.pdf (accessed on Jan 22, 2021).

[27] International Renewable Energy Agency, "Renewable energy technologies: cost analysis series, Wind Power", Available online: https://www.irena.org/-/media/Files/IRENA/Agency/Publication/2012/RE_Technologies_Cost_Analysis-WIND_POWER.pdf (Accessed on Jan, 22 2021)

[28] F. Spertino, S. Fichera, A. Ciocia, G. Malgaroli, P. Di Leo, and A. Ratclif, "Toward the complete self-sufficiency of an NZEBS microgrid by photovoltaic generators and heat pumps: Methods and applications," IEEE Trans. Ind. Appl., 2019, doi: 10.1109/TIA.2019.2914418.

[29] Corless, R.M., G.H. Gonnet, D.E.G. Hare, D.J. Jeffrey, and D.E. Knuth. "On the Lambert W Function." Advances in Computational Mathematics, Vol. 5, pp. 329–359, 1996.

[30] Jinko Solar, "Modules datasheets." https://www.jinkosolar.com/en/site/tigerpro (accessed May 10, 2020).

[31] Trina Solar, "Modules datasheets." https://www.trinasolar.com/en-glb/product/utility (accessed May 10, 2020).

[32] QCELLS, "Manufacturer of PV modules, Available online. https://www.q-cells.com/en/main/products/solar_panels/G5/g5_series01.html (accessed Jan. 20, 2021).

[33] Chicco, G.; Cocina, V.; Di Leo, P.; Spertino, F.; Massi Pavan, A. Error Assessment of Solar Irradiance Forecasts and AC Power from Energy Conversion Model in Grid-Connected Photovoltaic Systems. *Energies* 2016, *9*, 8.

[34] IKS Photovoltaic, "Manufacturer of measurement systems", Available online. http://www.iks-photovoltaik.de/fileadmin/iks/pdf/ISET_Sensor_EN.pdf

[35] Tritec, "Manufacturer of measurement systems", Available online. https://tritec.rocketcdn.me/wp-content/uploads/2020/02/spektron-210-en.pdf

[36] G. Chicco, F. Corona, R. Porumb and F. Spertino, "Experimental Indicators of Current Unbalance in Building-Integrated Photovoltaic Systems," in *IEEE Journal of Photovoltaics*, vol. 4, no. 3, pp. 924-934, May 2014

[37] Danish wind industry association, "Danish wind industry association." http://drømstørre.dk/wp-content/wind/miller/windpower web/en/stat/unitsw.htm#roughness (accessed Sep. 04, 2020).

[38] Carullo, A., Ciocia, A., Malgaroli, G., Spertino, F.; An Innovative Correction Method of Wind Speed for Efficiency Evaluation of Wind Turbines, In processing for (2020) Acta IMEKO.

[39] Ciocia, A.; Amato, A.; Di Leo, P.; Fichera, S.; Malgaroli, G.; Spertino, F.; Tzanova, S. Self-Consumption and Self-Sufficiency in Photovoltaic Systems: Effect of Grid Limitation and Storage Installation. *Energies* **2021**, *14*, 1591.

[40] Ollas, P.; Persson, J.; Markusson, C.; Alfadel, U. Impact of Battery Sizing on Self-Consumption, Self-Sufficiency and Peak Power Demand for a Low Energy Single-Family House With PV Production in Sweden. In Proceedings of the 2018 IEEE 7th World Conference on Photovoltaic Energy Conversion (WCPEC), Waikoloa Village, HI, USA, 10–15 June 2018; pp. 0618–0623.

[41] Tutkun, N.; Çelebi, N.; Bozok, N. Optimum unit sizing of wind-PV-battery system components in a typical residential home. In Proceedings of the 2016 International Renewable and Sustainable Energy Conference (IRSEC), Marrakech, Morocco, 14–17 November 2016; pp. 432–436.

[42] European Centre for Medium-Range Weather Forecasts , ERA5 database, Available online: https://confluence.ecmwf.int/display/CKB/ERA5%3A+data+documentation (accessed on 07 June 2021).

[43] European Commission. Regulation 2017/2195 of 23 November 2017 Establishing a Guideline on Electricity Balancing C/2017/7774. Available online: http://data.europa.eu/eli/reg/2017/2195/oj (accessed on 20 January 2021).

[44] Burgio, A.; Menniti, D.; Sorrentino, N.; Pinnarelli, A.; Leonowicz, Z. Influence and Impact of Data Averaging and Temporal Resolution on the Assessment of Energetic, Economic and Technical Issues of Hybrid Photovoltaic-Battery Systems. *Energies* **2020**, *13*, 354.

[45] A. Carullo, F. Ferraris, A. Vallan, F. Spertino, F. Attivissimo, Uncertainty analysis of degradation parameters estimated in long-term monitoring of photovoltaic plants, Measurement, Vol. 55, 2014, pp. 641-649.

[46] A. Carullo, A. Castellana, A. Vallan, A. Ciocia, F. Spertino, Uncertainty issues in the experimental assessment of degradation rate of power ratings in photovoltaic modules, Measurement, Vol. 111, 2017, pp. 432-440. Irradiance G 1.3 % of reading and maximum offset of 7 W/m2.

[47] A. Carullo, A. Ciocia, P. Di Leo, F. Giordano, G. Malgaroli, L. Peraga, F. Spertino, A. Vallan, Comparison of Correction Methods of Wind Speed for Performance Evaluation of Wind Turbines, Proc. of 24th IMEKO TC-4 2020 International Symposium, Virtual Conference, 14-16 Sep., pp. 291-296.

[48] M. Jafari, M. Korpås, and A. Botterud, "Power system decarbonization: Impacts of energy storage duration and interannual renewables variability," Renew. Energy, 2020, doi: 10.1016/j.renene.2020.04.144.

[49] Jiachen Mao, Mehdi Jafari, and Audun Botterud. "Planning Low-carbon Distributed Power Systems: Evaluating the Role of Energy Storage." *arXiv preprint arXiv:2009.09325* (2020).

[50] "RES-Plat." https://res-plat.est.polito.it (accessed May 10, 2020).

[51] Global Wind Atlas. Available online: https:// https://globalwindatlas.info/, accessed on 27th February 2021.

[52] Red Eléctrica, Spanish Transmission System Operator. Available online: https://www.ree.es/en/datos/todate, accessed on 27th February 2021.

[53] IRENA (2018), Renewable Energy Outlook: Egypt, International Renewable Energy Agency, Abu Dhabi.

[54] P. Boccardo, E. Bompard, S. Corgnati, D. Grosso, A. Ciocia, F. Spertino, G. Fulli, Marcelo Masera, "Res exploitation in the Southern Mediterranean area: a perspective analysis at 2040," in ENEMED, Med & Italian Energy Report, 2020.

[55] European Network of Transmission System Operators for Electricity (ENTSO-E), Available online: https://www.entsoe.eu/data/map/, accessed on 27th February 2021.

[56] International Energy Agency(IEA), "IEA Statistics." https://www.iea.org/statistics/.EA Statistics. Available online: https://www.iea.org/reports/world-energy-outlook-2019, accessed on 27th February 2021.

[57] European Commission, A hydrogen strategy for a climate-neutral Europe, COM(2020) 301 final

[58] E. Arco, E. Bompard, C. Mosca, F. Profumo, "Electricity based energy corridors connecting North and South shores of the Mediterranean," in ENEMED, Med & Italian Energy Report, 2020.

[59] J., Mehdi, A. Botterud, A. Sakti. "Estimating revenues from offshore wind-storage systems: The importance of advanced battery models." Applied Energy 276 (2020): 115417.

[60] W. J Cole, A. Frazier. Cost projections for utility-scale battery storage. Tech. rep. National Renewable Energy Laboratory (NREL), Golden, CO (United States), 2019.

[61] A. De Vita et al., Technology pathways in decarbonization scenarios. In: Advanced

System Studies for Energy Transition (2018). Available online: https://ec.europa.eu/energy/sites/ener/files/documents/2018_06_27_technology_pathways_-_finalreportmain2.pdf, accessed on 27th February 2021.

[62] M. S. Javed, T. Ma, J. Jurasz, M. Y. Amin (2020). Solar and wind power generation systems with pumped hydro storage: Review and future perspectives, Renewable Energy, 148, pp. 176-192.